2-9-2024

Unmixing Detrital Zircon U-Pb Ages Reveals Tectonic and Climatic Depositional Influences on the Carboniferous Ansilta Formation, Calingasta-Uspallata Basin, Western Argentina

Joshua R. Malone

John Malone

John L. Isbell

David H. Malone
Illinois State University, dhmalon@ilstu.edu

John P. Craddock
Illinois State University

Recommended Citation

J.R. Malone, J.E. Malone, J.L. Isbell, D.H. Malone, J.P. Craddock, K.N. Pauls, "Unmixing detrital zircon U-Pb ages reveals tectonic and climatic depositional influences on the Carboniferous Ansilta Formation, Calingasta-Uspallata Basin, Western Argentina," Geoscience Frontiers, 15, no. 4 (2024): 101807. https://doi.org/10.1016/j.gsf.2024.101807.

Geoscience Frontiers 15 (2024) 101807

Contents lists available at ScienceDirect

Geoscience Frontiers

journal homepage: www.elsevier.com/locate/gsf

Research Paper

Unmixing detrital zircon U-Pb ages reveals tectonic and climatic depositional influences on the Carboniferous Ansilta Formation, Calingasta-Uspallata Basin, Western Argentina

J.R. Malone [a,*], J.E. Malone [b,c], J.L. Isbell [c], D.H. Malone [d], J.P. Craddock [d], K.N. Pauls [c]

[a] Department of Geological Sciences, Jackson School of Geosciences, University of Texas at Austin, Austin, TX 78712, USA
[b] Iowa Geological Survey, University of Iowa, Iowa City, IA 52240, USA
[c] Department of Geosciences, University of Wisconsin–Milwaukee, Milwaukee, WI 53211, USA
[d] Department of Geography, Geology and the Environment, Illinois State University, Normal, IL 61790-4400, USA

ARTICLE INFO

Article history:
Received 30 October 2023
Revised 7 January 2024
Accepted 4 February 2024
Available online 9 February 2024
Handling Editor: Stijn Glorie

Keywords:
Late Paleozoic Ice Age
Argentina
Calingasta-Uspallata Basin
Ansilta Formation
Detrital zircon provenance

ABSTRACT

The Late Paleozoic Ice Age (LPIA) was a principal control of sedimentation across Gondwana from the late Devonian through early Permian. We assess the hypothesis that glacial to interglacial transitions in western Argentina were the primary control influencing sediment routing patterns among the various Carboniferous-Permian basins in western Argentina. The Carboniferous Ansilta Formation consists of glaciomarine, nearshore, and fluvial systems deposited during the LPIA along the eastern margin of the Calingasta-Uspallata Basin in Argentina. The lower, glacially influenced succession of the Ansilta Formation records at least five glacial advances; the upper succession of consists of progradational shallow marine, deltaic, and fluvial strata. We combine 1225 new U–Pb zircon ages from six samples of the Carboniferous Ansilta Formation in the Calingasta-Uspallata Basin with 5864 U–Pb ages from 147 published samples in the *detritalPy-mix* forward mixture model to characterize provenance shifts. For the glacially influenced lower Ansilta Formation, sediment was derived locally from the Protoprecordillera, which was a prominent highland with alpine glaciers flowing west and east into the Calingasta-Uspallata and Paganzo basins, respectively. Thus, there was little or no connection between these two basins during Serpukhovian-Bashkirian glaciation. The fluvial/deltaic upper Ansilta had distal sediment sources in the Sierras Pampeanas. Furthermore, our results support the collapse of the Protoprecordillera topographic barrier, enabling drainage patterns connecting the Paganzo and Calingasta-Uspallata basins by late Pennsylvanian-early Permian time.

1. Introduction

The Late Paleozoic Ice Age (LPIA) involved numerous, temporally and spatially distinct glaciations throughout the southern hemisphere (López-Gamundí, 1997; Isbell et al., 2003, 2012, 2021; Fielding et al., 2008a, 2008b; Montañez and Poulsen, 2013; Cagliari et al., 2016, 2023; Griffis et al., 2018, 2019; Mottin et al., 2018, 2023; Craddock et al., 2019; López-Gamundí et al., 2021; Rosa and Isbell, 2021; Veroslavsky et al., 2021). Far-field effects of these glaciations are known in the northern hemisphere (e.g. Crowell, 1970; Veevers and Powell, 1987; Crowell, 1999; Isbell et al., 2003, 2012, 2016; Heckel, 2008, 2022; Rygel et al., 2008; Shi and Waterhouse, 2010; Kissock et al., 2018; Thomas et al., 2020).

Multiple episodes of alpine and continental glaciation are evident (López-Gamundí, 1997; Isbell et al., 2003; Craddock et al., 2019; López-Gamundí et al., 2021; Rosa and Isbell, 2021). In northern Brazil, Peru, Bolivia, and Argentina, glaciation began during the Famennian and expanded through western Gondwana during the Tournissian and Visean (e.g., Caputo and Crowell, 1985; Díaz-Martínez et al., 1999; Caputo et al., 2008; Isaacson et al., 2008; Playford et al., 2012; Caputo and Santos, 2020; López-Gamundí et al., 2021). The first glacial acme occurred during the Serpukhovian-Bashkirian (~327–318 Ma) with evidence of glaciation in southern Bolivia, western Argentina, the Paraná Basin, the Solimões and Amazonas basins in Brazil, possibly southern Africa, and in eastern Australia followed by sporadic glaciation throughout the rest of the Pennsylvanian (López-Gamundí et al., 1987,

* Corresponding author.
E-mail addresses: joshua.malone@utexas.edu (J.R. Malone), john-malone@uiowa.edu (J.E. Malone), jisbell@uwm.edu (J.L. Isbell), dhmalon@ilstu.edu (D.H. Malone).

https://doi.org/10.1016/j.gsf.2024.101807

2021; Limarino et al., 2002; Fielding et al., 2008a,b; Henry et al., 2008; Gulbranson et al., 2010; Rosa et al., 2019; Pauls et al., 2021; Rosa and Isbell, 2021; Correa et al., 2022; Malone et al., 2023a). A second glacial acme recorded by glaciogenic strata across Gondwana occurred during the late Pennsylvanian-early Permian, with records in the Paraná Basin, Falkland/Malvinas Islands, Ventana Fold belt in South America, Karoo and Kalahari basins in Southern Africa, Antarctica, India, the Arabian Peninsula, Australia, and in dispersed terranes now located in southern Asia (Visser, 1987, 1989, 1997; von Brunn, 1996; Trewin et al., 2002; Fielding et al., 2008a, 2008b, 2022; Isbell et al., 2008a, 2008b; Rocha-Campos et al., 2008; Martin et al., 2012, 2019; Mory, 2017; Horan et al., 2018; Craddock et al., 2019; An et al., 2023; Choudhuri et al., 2023; Malone et al., 2023b). Glaciation continued in South Africa until the middle Permian, and until the late Permian in Eastern Australia (Griffis et al., 2019; Fielding et al., 2022).

Recent work in the various South American basins has refined the LPIA into five short glacial episodes (López-Gamundí et al., 2021). These are the Famenian-Tournaisian "Event 1" recorded in the Tarija, Chaco-Parana and Río Blanco basins, the Tournaisian "Event 2" evident in the Calingasta-Uspallata Basin, the Visean "Event 3" interpreted in the Calingasta-Uspallata, Tarija, Chaco-Paraná basins, the Serpukhovian-Bashkirian "Event 4" that occurred throughout southwestern Gondwana, and the Pennsylvanian-early Permian "Event 5", which occurred extensively throughout eastern South America in the linked Paraná, CChaco-Paraná, Norte, Claromecó/Sauce Grande/Ventana fold belt basins (Fig. 1).

Diamictites occur in the late Paleozoic basins and paleovalleys of Argentina, Brazil, Uruguay, Paraguay, and Bolivia (López-Gamundi and Buatois, 2010; Limarino et al., 2014a; Isbell et al., 2023; Fig. 1). In west-central Argentina, Serpukovian-Bashkirian proximal to distal glaciomarine and rare subglacial deposits occur in the Calingasta-Uspallata, Paganzo, and Río Blanco basins (López-Gamundí et al., 1987, 2016; Henry et al., 2008, 2010; Aquino et al., 2014; Alonso-Muruaga et al., 2018; Valdez Buso et al., 2020; Pauls et al., 2021; Correa et al., 2022; Malone et al., 2023a). The Calingasta-Uspallata Basin stratigraphic succession, including the Agua de Jagüel, Hoyada Verde, Leoncito, Majaditas, El Paso and Ansilta formations, many of which occur in paleovalleys, provide ample evidence of glacially influenced sedimentation. Various palaeontologic methods and the dating of ash beds have been used to establish biostratigraphic correlations among these widely separated successions (Fig. 2; Césari and Gutiérrez, 2001; Taboada, 2004, 2009; Gulbranson et al., 2010; Césari et al., 2011, 2014, 2021; Valdez Buso et al., 2017).

Although strata in the Paganzo Basin to the east and the Río Blanco Basin to the north (Gulbranson et al., 2010; Césari et al., 2019; Valdez Buso et al., 2021) have some geochronologic control (Césari and Gutiérrez, 2001; Taboada, 2004, 2009, 2010; Césari et al., 2011, 2014; Limarino et al., 2014a; Pauls et al., 2021), such control for the Calingasta-Uspallata Basin is not yet established. The lower Ansilta Formation in the Calingasta-Uspallata Basin in Leoncito National Park consists of a lower diamictite-bearing succession that was deposited during the late Serpukhovian to early Bashkirian western Gondwana glacial maximum. The upper succession of the Ansilta Formation here includes shallow marine, deltaic, and fluvial strata that may be as young as the early Permian (Isbell et al., 2003, 2012, 2021; Gulbranson et al., 2010; Césari et al., 2014; Limarino et al., 2014b; López-Gamundí et al., 2021; Rosa and Isbell, 2021; Malone et al., 2023a). Taboada (2010) characterized the lower Ansilta diamictite interval and the overlying non-glacial nearshore succession as being Serpukhovian-Bashkirian due to the presence of *Nothorhacopteris–Botrychiopsis–Ginkgophyllum* (NBG biozone) flora and post-glacial fauna. Césari et al. (2014) identified Permian flora in fluvial strata from the top of the upper succession, which places an early Cisuralian age for the uppermost boundary.

Detrital zircon U–Pb geochronology is an important application for determining sedimentary provenance and for understanding Carboniferous sediment dispersal patterns in Gondwana (e.g., Craddock et al., 2019; Pauls et al., 2021; Ives et al., 2022; Malone et al., 2023b) and globally (e.g. Kissock et al., 2018; Thomas et al., 2020). This paper presents a detailed provenance analysis of the Ansilta Formation of the northern part of the Calingasta-Uspallata Basin (Fig. 1); it is based on the facies and sequence stratigraphic analysis of this same section (Malone et al., 2023a). By integrating these near- (i.e., sequence stratigraphy and facies sedimentology) and far-field (detrital zircon U–Pb geochronology) proxies, we provide new insights into the glacial dynamics and paleogeographic setting for NW Argentina during and after the mid-Carboniferous boundary of the LPIA (Isbell et al., 2021; López-Gamundí et al., 2021). Our aim is to assess the provenance of the Ansilta Formation to better understand the nature, location, and extent of glaciation, and determine whether sediments were sourced locally, or if a distal ice sheet or ice cap further to the east fed ice into the Ansilta paleovalley of the Protoprecordillera. Specifically, the scientific questions that we address are:

(1) Is the glacially influenced succession of the lower Ansilta Formation sourced locally from the present Precordillera or is a distal eastern sediment source observable? The implications of the former would permit the interpretation that the Protoprecordillera was a prominent highland with alpine glaciers flowing east and west into the Calingasta-Uspallata and Paganzo basins, respectively. This would imply that the Calingasta-Uspallata and Paganzo basins were not connected in this section of the range during the mid-Carboniferous glaciation, and that glaciation may have been limited to uplifts in the Protoprecordillera with other uplifts in the western Paganzo Basin also housing ice caps of alpine glaciers (Limarino and Gutierrez, 1990; Henry et al., 2008; Columbi et al., 2018; Craddock et al., 2019; Pauls et al., 2021), rather than continental in scale at that time. A distal eastern sediment source for the lower Ansilta Formation would permit the interpretation that continental-scale glaciation occurred, with an ice dome further to the east overlying the eastern Sierra Pampeanas, Rio de La Plata Craton, eastern Africa, or Antarctica. This hypothesis is supported by the work of Starck et al. (2021) who identified Paleoproterozoic granite boulders in Pennsylvanian diamictite in the Tarija basin to the north. These boulders must have been sourced more than 1000 km to the east in the Rio de la Plata craton, which is similar in scale to what was reported by Malone et al. (2022) for the Laurentide glaciations of North America. Starck et al. (2021), however, ignore the occurrence of Paleoproterozoic granitic rocks located much closer to the site of that study. Geologic maps show rocks of this age north of Concepción, Paraguay and possibly underlying the thick Cenozoic package that blank eastern Bolivia and western Paraguay, both of which are located less than 500 km away to the east (Gómez Tapias, 2019). In addition, Milana and Di Pasquo (2019, 2023) record significant relief along the basal erosional surface and a lack of onlapping glacial deposits within the paleovalley of the Del Salto Formation in the western Precordillera as well as inferred deposition of the Tontal section being near sea level without influence of a prominent topographic feature. This examination of strata in the northern Calingasta-Uspallata basin led them to the interpretation of a more extensive Serpuhkovian-Bashkirian glaciation that drained through the Precordillera and covered the Paganzo basin and large areas to the east. Their examination ignored other paleovalleys in the Precordillera, some of which drain to the east that contain mid-Carboniferous glaciogenic strata and are over 1000 m deep (Kneller et al., 2004; Dykstra et al., 2006; Henry et al., 2010; Aquino et al., 2014; Alonso-Muruaga et al., 2018).

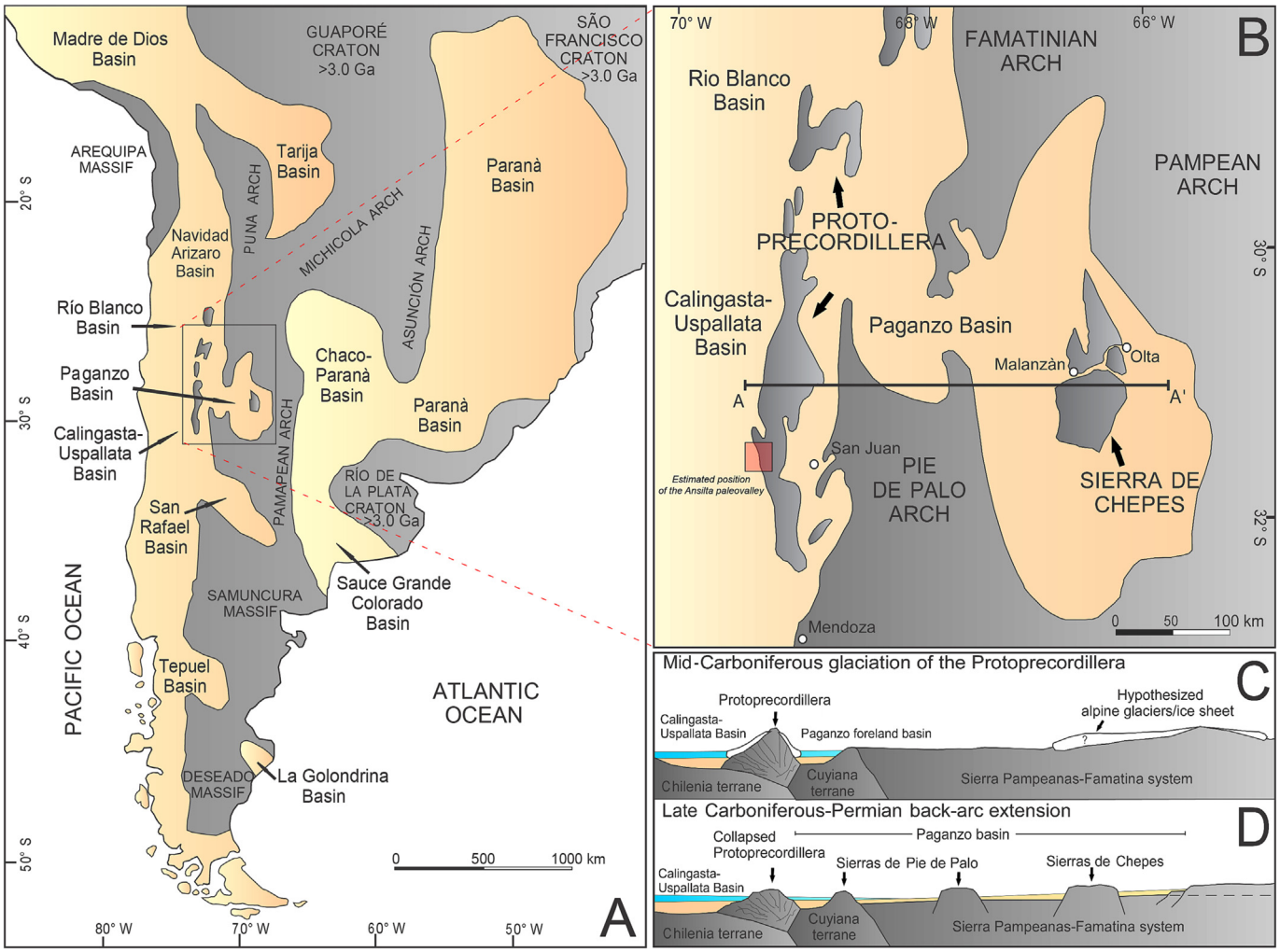

Fig. 1. (A) Regional map of the distribution of late Paleozoic basins and interpreted basement paleotopographic highs in South America. Modified from Henry et al. (2010), Moxness et al. (2018) and Malone et al. (2023a). (B) Map of the Precordillera and adjacent basins. Red shaded box is the study area. (C-D) Cross sections of the principal late Paleozoic tectonic, sedimentary, and cryogenic features. (For interpretation of the references to color in this figure legend, the reader is referred to the web version of this article.)

(2) Does the detrital zircon U–Pb provenance of the Ansilta Formation shift following the transition from glacially influenced to marginal marine deposition corresponding to the sequence stratigraphic and facies changes interpreted by Malone et al. (2023a). No provenance change would indicate that the Protoprecordillera remained a prominent topographic and sediment barrier throughout Ansilta deposition here. Correa et al. (2022), based on biostratigraphic and sedimentological evidence within strata of the Calingasta-Uspallata basin, interpret that the Protoprecordillera collapse occurred during the latest Pennsylvanian to early Permian time and coeval with the height of distal latest Pennsylvanian to early Permian continental-scale glaciation. Therefore, if the upper Ansilta Formation was sourced from distal eastern sources (Sierras Pampeanas and/or Famatinian arc, and perhaps the Rio de la Plata craton), this would imply a collapse of the Protoprecordillera and enable sediment to be delivered to the Calingasta-Uspallata Basin.

2. Geologic setting

2.1. Regional geologic framework

The western Gondwanan margin of present-day Argentina consists of an assemblage of accreted terranes (Pampia, Cuyania, and Chilenia), igneous intrusions, and subsequent metamorphosed units (Ramos, 1988; Pankhurst et al., 1998; Ramos et al., 1998, 2015; Rapela et al., 1998, 2007; Rapalini, 2005; Dahlquist et al., 2010). The Pampia terrane, also known as the Sierras Pampeanas, accreted to the Gondwanan margin during the Neoproterozoic to Cambrian (Rapela et al., 1998, 2007; Rino et al., 2008; Ramos et al., 2015). The Sierras Pampeanas are subdivided into two regions: (1) Eastern Sierras Pampeanas, (2) Western Sierras Pampeanas (see discussion below). Westward of the Pampia terrane lies the Cuyania terrane, which rifted from southern Laurentia during the latest Neoproterozoic- Cambrian (Kay et al., 1996; Keller et al., 1998; Keller, 1999; Casquet et al., 2001, 2012; Ramos, 2004; Freiburg et al., 2022) and accreted to the western margin of Gondwana between 460 Ma and 435 Ma. Much of the Grenville-age (1.2–1.0 Ga) crystalline basement within the Cuyania terrane (Kay et al., 1996; Thomas and Astini, 1996; Martin et al., 2020) is overlain by Neoproterozoic, Cambrian, Ordovician, and Silurian strata (Huff et al., 1998; Keller, 1999; Dahlquist et al., 2010; Naipauer et al., 2010; Verdecchia et al., 2011, 2014; Casquet et al., 2012; Sial et al., 2013), however, this region was intruded by the Ordovician Famatinian magmatic belt emplaced from 490 Ma to 450 Ma, with the main magmatism occurring between 490 Ma and 470 Ma (Pankhurst et al., 1998, 2000; Ramos et al., 1998;

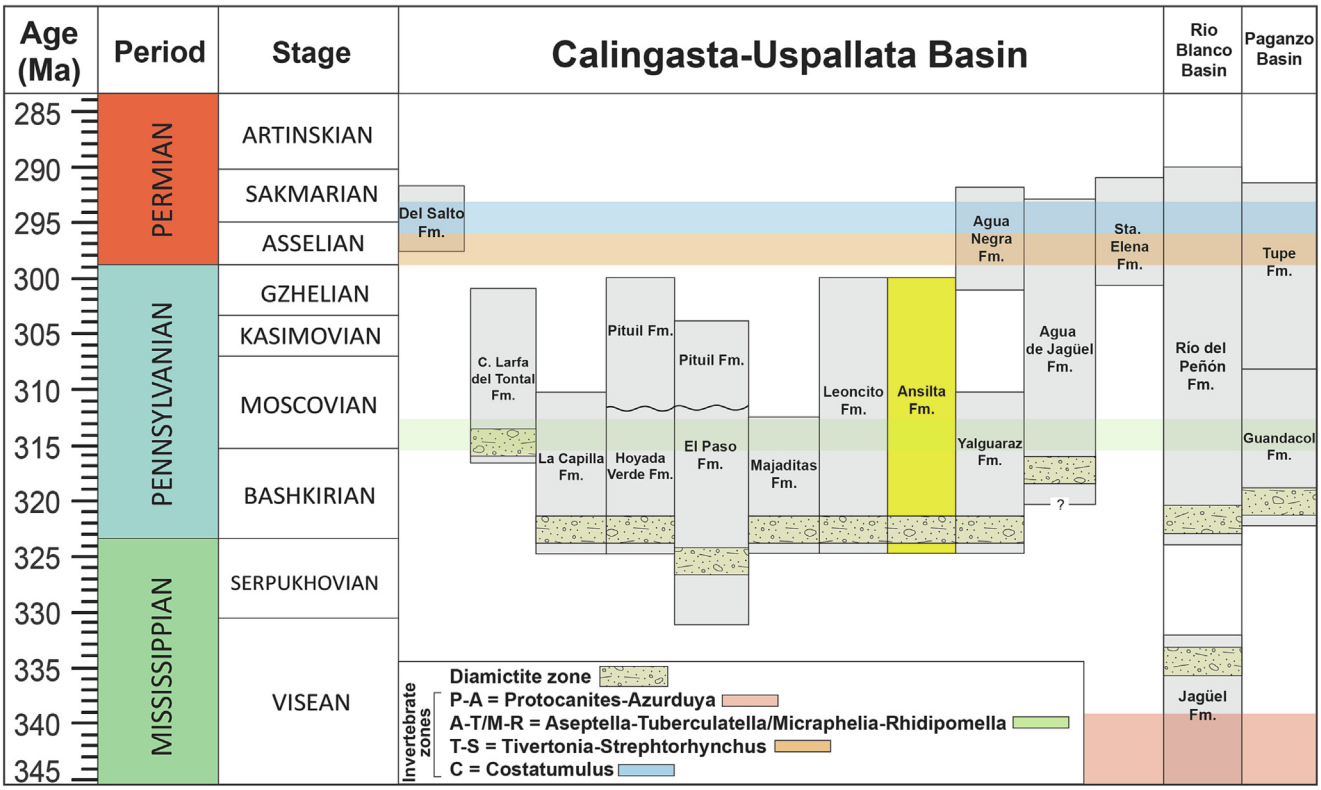

Fig. 2. Correlation of late Paleozoic sedimentary units in the Calingasta-Uspallata Basin displaying the time and occurrence of diamictite zones. Yellow highlight is the formation of focus for this study. Modified after López-Gamundí et al. (1987), Taboada (2004, 2010), Henry et al. (2010). Biostratigraphic zones are provided. (For interpretation of the references to color in this figure legend, the reader is referred to the web version of this article.)

Ramos, 1999; Rapela et al., 2018; Larrovere et al., 2021). The N–S trending Famatinian magmatic belt is interpreted as a marginal arc that developed as Cuyania converged on the Argentine region of Gondwana (Pankhurst et al., 1998, 2000; Vujovich and Ostera, 2003; Dahlquist et al., 2010; Enkelmann et al., 2014; Ducea et al., 2015). Post orogenic Devonian to early Carboniferous granites intruded into the Famatina magmatic belt (365–345 Ma; Pankhurst et al., 1998; Dahlquist et al., 2010; Martina et al., 2018).

The accretion of the Chilenia terrane during the middle Devonian to early Mississippian resulted in the Chañic orogeny, resulting in the exhumation of the Protoprecordillera (Ramos et al., 1984, 1986; Limarino et al., 2006; Arnol et al., 2022; Dahlquist et al., 2022; García-Sansegundo et al., 2023). Prior to accretion, strata of the Precordillera existed as a thick succession of deep marine siliciclastic rocks, which were part of an accretionary prism (Thomas et al., 2015; Ariza et al., 2018). Post-collisional orogenic collapse of the Protoprecordillera occurred during the Carboniferous as subduction shifted westward, enabling this region to evolve into an intra-arc basin.

2.2. Late Paleozoic ice age (LPIA)

The extent and duration of the glacial episode(s) throughout the LPIA have been the focus of hundreds of studies, most recently summarized by Henry et al. (2010), Rosa and Isbell (2021), López-Gamundí et al. (2021), and Montañez (2022). While some propose the idea of a single continental-scale ice sheet covering southern Gondwana (Scotese and Barrett, 1990; Starck and Del Papa, 2006; Starck et al., 2021), others propose several smaller, disconnected, ice centers dispersed around Gondwana (Isbell et al., 2012, 2021; Montañez and Poulsen, 2013; Griffis et al., 2019; López-Gamundí et al., 2021). The principal drivers of LPIA glaciations include long-term tectonic raising and lowering of the equilibrium-line altitude (Isbell et al., 2012; Montañez and Poulsen, 2013), migration of Gondwana across the South Pole resulting in shifting glacial centers (Caputo and Crowell, 1985; Scotese and Barrett, 1990), perturbations in global CO_2 levels (Montañez et al., 2016), explosive volcanism (Soreghan et al., 2019), and the trapping of humid air masses (Pauls, 2020; Dávila et al., 2021; Pauls et al., 2021). Late Paleozoic strata in western-Argentina constrain at least two glacial episodes, each spanning about 8 m.y.: Visean-early Serpukhovian and late Serpukhovian-early Bashkirian (César et al., 2011; Rosa and Isbell, 2021). During these episodes, alpine glaciers radiated from the Protoprecordillera into both the Calingasta-Uspallata and Paganzo basins (López-Gamundí et al., 1994; Dykstra et al., 2006; Limarino et al., 2006; Henry et al., 2010; Aquino et al., 2014; Valdez Buso et al., 2017, 2020; Milana and Di Pasquo, 2019; Pauls, 2020; Pauls et al., 2021; Correa et al., 2022; Malone et al., 2023a). Evidence for this model are paleovalleys with > 1000 m of relief that contain glaciogenic strata deposited by tidewater glaciers (López-Gamundí, 1986; Kneller et al., 2004; Henry et al., 2008, 2010; Aquino et al., 2014; Limarino et al., 2014a; López-Gamundí et al., 2016; Valdez Buso et al., 2017, 2020; Alonso-Muruaga et al., 2018; Moxness et al., 2018; Pauls et al., 2021; Malone et al., 2023a). Some of these paleovalleys enabled drainage toward the sea to the west, while through going valleys allowed marine transgressions toward the continent.

2.3. Ansilta Formation

The Ansilta Formation study area is located 5 km southeast of the Astronomical Observatory El Leoncito near Barreal, San Juan Province, Argentina (Fig. 1). Here the Ansilta consists of a lower

glaciomarine succession, and an upper nearshore to fluvial-deltaic succession deposited during the LPIA along the eastern margin of the Calingasta-Uspallata Basin (Malone et al., 2023a). The Ansilta Formation unconformably overlies the Upper Ordovician to Lower Silurian Hilario and Cabeceras formations and is overlain by the Permo-Triassic Santa Clara Group (Csaky, 1963; Amos and Rolleri, 1965; Fig. 3).

Several researchers (Amos and Rolleri, 1965; Harrington, 1971; Amos and López-Gamundí, 1981; De Rosa, 1983; López-Gamundi, 1987; López-Gamundí and Martínez, 2003; Henry et al., 2008, 2010; López-Gamundí et al., 2010, 2016; Limarino et al., 2011; Correa et al., 2022; Malone et al., 2023a) provide excellent descriptions of late Paleozoic diamictite-bearing strata exposed in the Calingasta-Uspallata basin. The Ansilta Formation was originally defined by Harrington (1971) as a ~ 700 m thick succession that includes the diamictite-bearing strata of the Calingasta-Uspallata Basin. Prior to that, Amos and Rolleri (1965) informally subdivided this succession into lower, middle, and upper sections. López-Gamundí (1986) provided the first detailed sedimentological analysis of the lower and middle Ansilta Formation. Taboada (2004, 2010) provided a detailed biostratigraphic analysis of the unit and recognized post-*Levipustula* faunas in the lower glacial succession (Malone et al., 2023a sequences 1–5; Fig. 3) and the upper post-glacial succession (sequences 6–8), which places an uppermost Bashkirian age limit through the top of sequence 8. Césari et al. (2014) identified Permian plant remains of conifers and glossopterids at the top of the upper succession (Sequences 9–10; Fig. 3), signifying that the uppermost portion of the Ansilta Formation is Asselian or younger. Thus, prior to the onset of our work here, two depositional successions were identified in the Ansilta Formation, consisting of a lower glaciogenic succession and an upper shallow marine and fluvial succession. The lower succession of the Ansilta formation is correlative with other glaciogenic strata elsewhere in the basin, is greater than 425 m thick, and is composed of diamictite, conglomerate, sandstone, pebbly mudstone, and shale (López-Gamundi, 1987; Taboada, 2004; Césari et al., 2014).

Malone et al. (2023a; Figs. 3–4) placed the Ansilta Formation in a sequence stratigraphic context and interpreted that the lower glacially influenced succession (0–427 m) records at least five glacial advances. The upper succession of the Ansilta Formation (427–700 + m) consists of at least additional five siliciclastic sequences of progradational shallow marine shelf, deltaic, and fluvial strata.

3. Methodology

3.1. Sample collection and preparation

This study expands upon J.E. Malone et al. (2023a) which provided a sequence stratigraphic framework of a ~ 700 m measured section of the lower Ansilta Formation, located 5 km southeast of the Leoncito Observatory in Leoncito National Park (−31.832014, −69.244178). Six samples collected in the field were crushed and processed for detrital zircon geochronology (n = 1225 total zircons analyzed). Sampling horizons included the underlying early Paleozoic basement (CU19-2), three sandstone lenses within the diamictite-bearing portion of the lower succession (Fig. 4; CU19-1, CU19-5, CU19-7), and two sandstones from the upper shallow marine and fluvial succession (Fig. 4; CU19-10, CU19-11). We also include detrital zircon data from the Tupe (Pauls, 2020; n = 72) and Guandacol (Pauls et al., 2021; n = 76) formations of the Paganzo Basin.

Zircon crystals are extracted from ~ 5 kg samples by traditional methods of crushing and grinding, followed by separation with a Wilfley table, heavy liquids, and a Frantz magnetic separator. Samples are processed such that all zircons are retained in the final

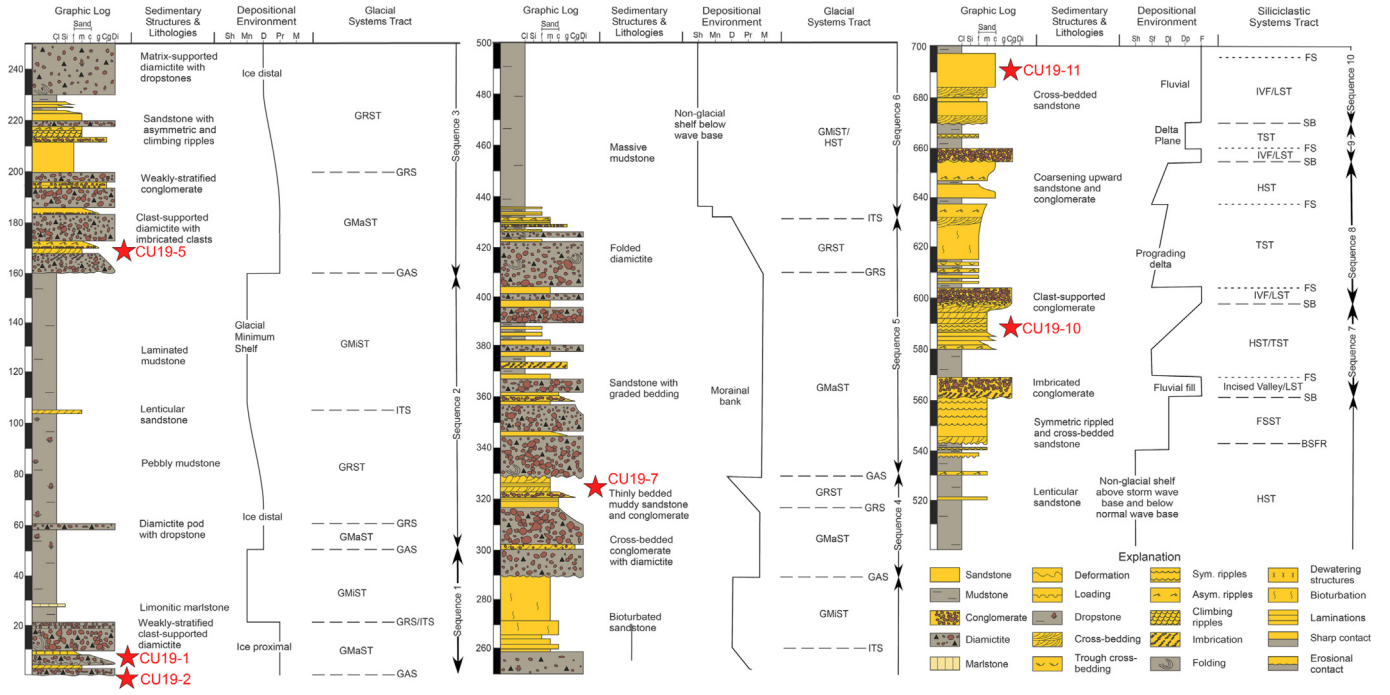

Fig. 3. Stratigraphic column, system tracts, and interpreted depositional processes for the lower (sequence 1–5) and upper (sequence 6–10) Ansilta Formation. Symbols across the top for depositional environments include: Sh = Non-glacial shelf; Mn = Glacial minimum; D = Ice distal; Pr = Ice proximal; M = Morainal bank; Sf = Shoreface; Dl = Delta; Dp = Delta plain; F = Fluvial. System tract and bounding surface nomenclature include: GAS = Glacial Advance Surface; GMaST = Glacial Maximum Systems Tract; GRS = Glacial Retreat Surface; ITS = Iceberg Termination Surface; GMiST = Glacial Minimum Systems Tract; GRST = Glacial Retreat Systems Tract; SB = Sequence Boundary; MRS = Maximum Retreat Surface; MFS = Maximum Flooding Surface; TST = Transgressive Systems Tract; HST = Highstand Systems Tract; BSFR = Basal Surface of Forced Regression; FSST = Falling Stage Systems Tract; IVF = Incised Valley Fill; LST = Lowstand Systems Tract; FS = Flooding Surface. Sample locations are indicated.

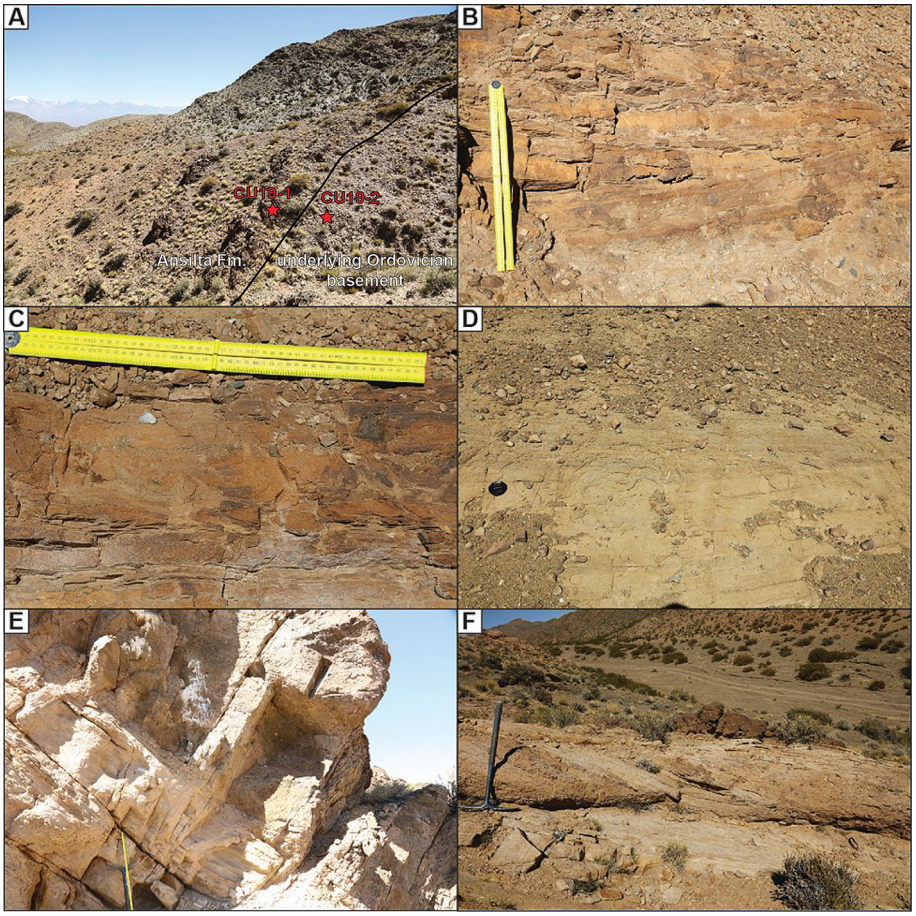

Fig. 4. Photo mosaic of sampled lithologies from the Ansilta Formation. (A) Basal contact between Ansilta Formation and underlying Ordovician basement, with CU19-2 sampled from basement rocks. (B) Sample CU19-1 was collected from sandstone within diamictite in sequence 1. Ruler (0.5 m) for scale. (C) Sample CU19-5 comes from sandstone with soft sediment deformation structures near the base of sequence 3. Ruler (0.5 m) for scale. (D) Sample CU19-7 collected from interlayered conglomerate and sandstone at the top of sequence 4. Camera lens (7 cm) for scale. (E) Sample CU19-10 comes from a coarsening upward succession of sandstone and conglomerate at the top of sequence 7. Ruler (1 m) for scale. (F) Sample CU19-11 collected from sandstone foresets from sequence 10. Geology pick (1 m) for scale.

heavy mineral fraction. A large split of grains (thousands of grains) is incorporated into a 1″ epoxy mount together with fragments or loose grains of Sri Lanka, FC-1, and R33 zircon crystals as the zircon standards. The mounts are sanded down to a depth of ~ 20 μm, polished, imaged, and cleaned prior to isotopic analysis.

Grains of interest are imaged to provide a guide for locating analysis pits in optimal locations, and to assist in interpreting results. BSE and color CL Images are generated with a Hitachi 3400 N SEM and a Gatan CL2 detector system (https://www.geoarizonasem.org).

U–Pb geochronologic analyses were conducted by laser ablation inductively coupled plasma mass spectrometry (LA-ICPMS) at the Arizona LaserChron Center (https://www.laserchron.org). Methods for U–Pb geochronology have been described by Gehrels et al. (2006, 2008), Gehrels and Pecha (2014), and Pullen et al. (2018). The analyses involve ablation of zircon with a Photon Machines Analyte G2 excimer laser equipped with HelEx ablation cell using a spot diameter of 20 μm. Data reduction was conducted using AgeCalcML software (Sundell et al., 2021). Analyses with > 20% discordance, >5% reverse discordance, or > 10% internal (measurement) uncertainty were excluded. Further details of the analyses are included in the Supplementary Data file.

3.2. Multidimensional scaling

Given a table of pairwise 'dissimilarities', the MDS technique utilizes principal component analysis (PCA) and produces a dimensionless map of points on which samples with statistically similar age distributions cluster close together and statistically dissimilar samples plot farther apart (Vermeesch, 2012). MDS plots were constructed with DZmds (Saylor et al., 2019) using probability density plot cross-correlation and the optimum number of dimensions to reduce stress. The probability density plot cross-correlation MDS approach can be sensitive to a sample size below n = 300 (Saylor and Sundell, 2016), but provides the most dependable method for assessing similarity among multiple samples (Saylor and Sundell, 2016).

3.3. Kolmogorov-Smirnov (K-S) statistics

The K-S test utilized in this study follows the approach used by Craddock et al. (2019), which compares two sample age distributions to determine if there is a statistically significant difference between them. The fundamental measure for the K-S test is the P value: if the P-value is < 0.05, the level of confidence that the two age distributions are not the same (do not share similar provenance) is > 95%.

3.4. Forward mixture modeling

We used a temporal approach to characterize eleven potential sources terranes (parents) believed to contribute in varying proportions to produce each measured basinal (child) age distribution. Because of the complexity of the accretionary tectonic history,

there is spatial overlap to these sedimentary, tectonic, and magmatic events, with a gradual increase in age in source terranes to the east. We compiled 5864 magmatic and detrital U–Pb detrital zircon ages from 147 published samples to characterize eleven source terranes in west-central South America believed to be principal sediment sources for the Ansilta Formation (DZ_Mix_-Comp_FINAL in the Supplemental Data files; Fig. 5–Fig. 6). These are (1) Rio de la Plata craton, (2) Western Precordillera, (3) Central Precordillera, (4) Eastern Precordillera, (5) Western Sierras Pampeanas, (6) Eastern Sierras Pampeanas, (7) Famatinian belt, (8) Paleozoic accretionary complex, (9) Devonian arc, (10,11) Carboniferous retro-arc, and (11) Carboniferous magmatic arc domains.

Forward mixture modeling was completed using *detritalPy-mix*, a new update to detritalPy toolkit (Sharman et al., 2018), that determines a best-fit mixture and estimates uncertainty and model goodness-of-fit through a 'bootstrapping' technique (Malkowski et al., 2019, 2022). The 'bootstrapping' approach characterizes the uncertainty associated with the best-fit models. Each parent and child distribution (with replacement) were resampled for one thousand iterations, providing a characterization of the distribution of the best fitting mixture modelled child distributions and best fitting D_{max} values (Fig. 7A). To properly determine if the 'best-fit' is a 'good-fit', a second resampling experiment was performed, which resampled the child (with replacement) and then was compared to the original observation. The second resampling experiment enables the visualization of the variability in the observed child (due to sampling) and the range of D_{max} values expected for comparison between two samples drawn from the child sample (Fig. 7B, 7C). A model with a 'good-fit' has a large overlap between the bootstrapped model comparisons and bootstrapped self-comparisons.

The details of the LA-ICPMS U–Pb data, and the compiled data for the *detritalPy-mix* are included in the Supplementary Data files.

4. Results

4.1. U–Pb geochronology

We report 1225 new U–Pb ages from detrital zircons from five samples within the Carboniferous Ansilta Formation in the Calingasta-Uspallata Basin (Fig. 7A). A sixth sample (CU19-2; n = 211) collected from the underlying Ordovician strata and has zircons that range in age from 2794 Ma to 451 Ma. The detrital zircon age mode is Mesoproterozoic (1099 Ma), with a lesser mode of Ordovician age (470 Ma). The detrital zircon age spectrum for sample CU19-1 (n = 101; 9 m from base), collected from a sandstone layer within the diamictite-bearing succession near the base of sequence 1, ranges from 2043 Ma to 321 Ma. Detrital zircon age modes for sample CU19-1 are 1170 Ma, 1078 Ma, 453 Ma and 365 Ma. Sample CU19-5 (n = 215; 168 m from base) comes from a sandstone lens within a diamictite-bearing section from the bottom of sequence 3 (Fig. 3). The detrital zircon age spectrum ranges from 2702 Ma to 331 Ma and has a primary Chañic age mode of

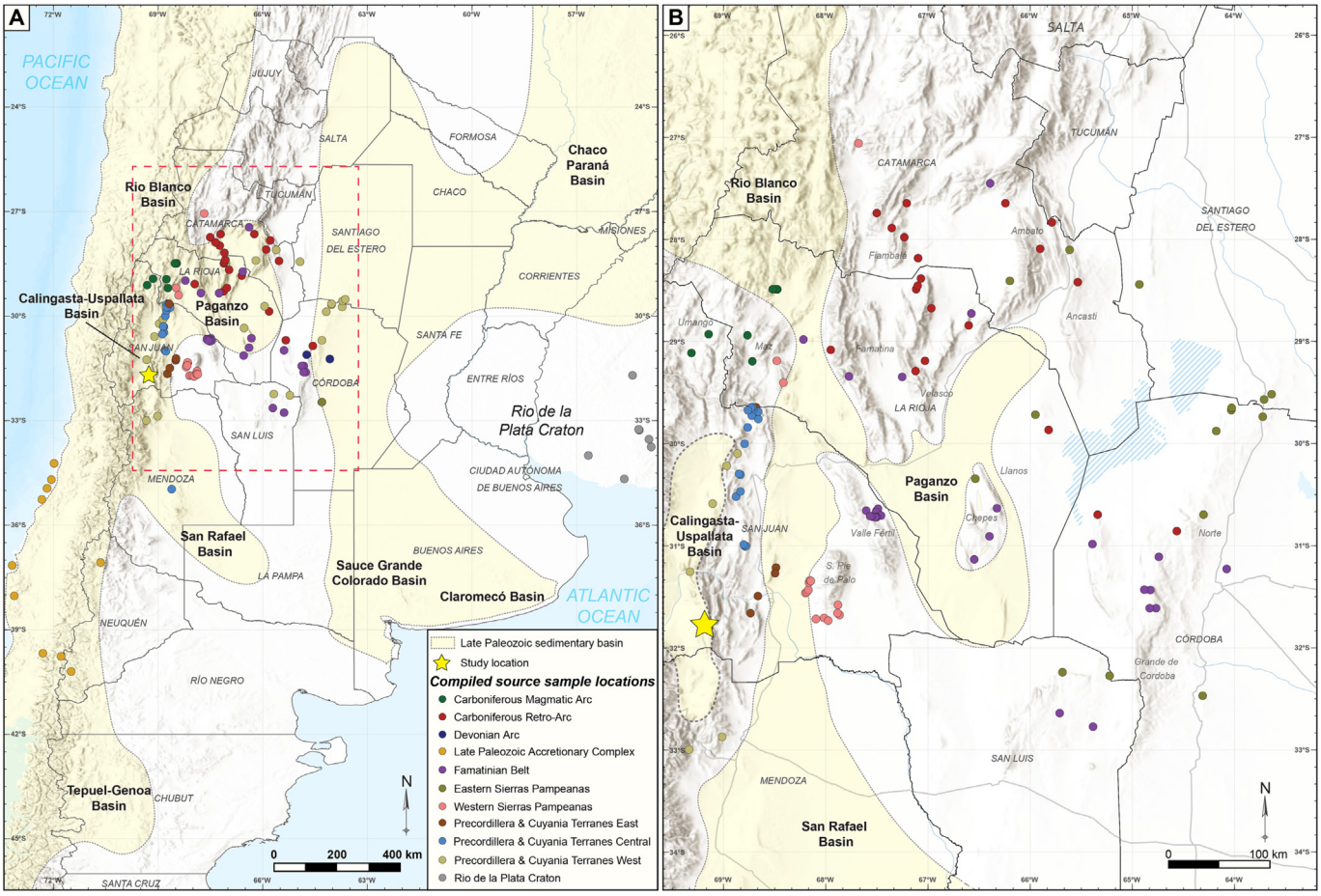

Fig. 5. (A) Regional map of southern South America showing the eleven principal source terranes capable of supplying detritus to west-central Argentina during the late Paleozoic. Individual dots represent compiled individual source data used to characterize specific source regions. (B) Overview of individual sources within the Sierra Pampeanas in west-central Argentina.

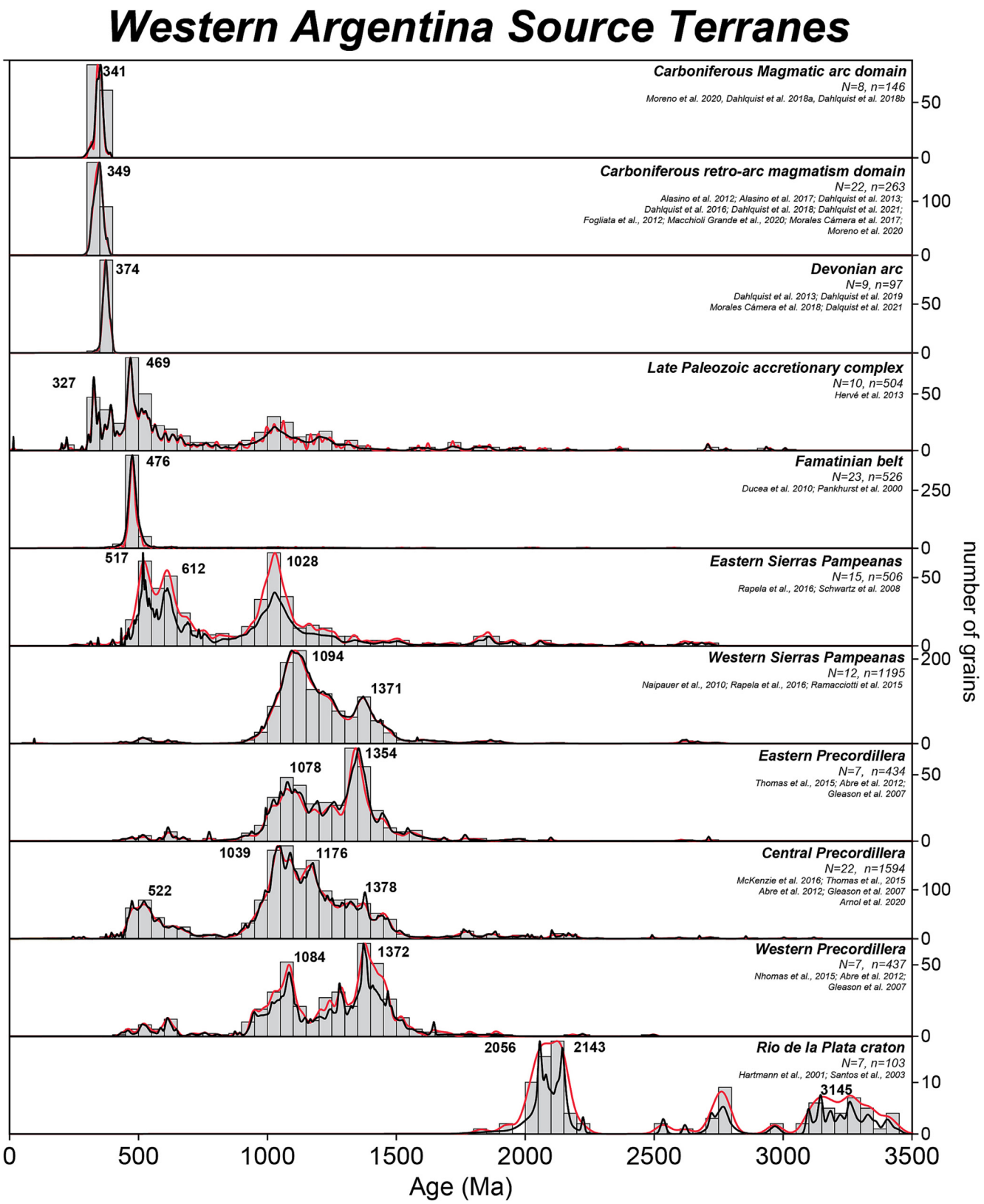

Fig. 6. Compiled detrital and magmatic zircon U-Pb ages (N = 159, n = 5441) across the eleven proposed source terranes in west-central Argentina: (1) Rio de la Plata craton, (2) Western Precordillera, (3) Central Precordillera, (4) Eastern Precordillera, (5) Western Sierras Pampeanas, (6) Eastern Sierras Pampeanas, (7) Famatinian belt, (8) Paleozoic accretionary complex, (9) Devonian arc, and (10,11) Carboniferous *retro*-arc and magmatic arc domains. Note: histogram bin width = 50 Ma; kernel density estimate (KDE) = red line; probability density plot (PDP) = black line. (For interpretation of the references to color in this figure legend, the reader is referred to the web version of this article.)

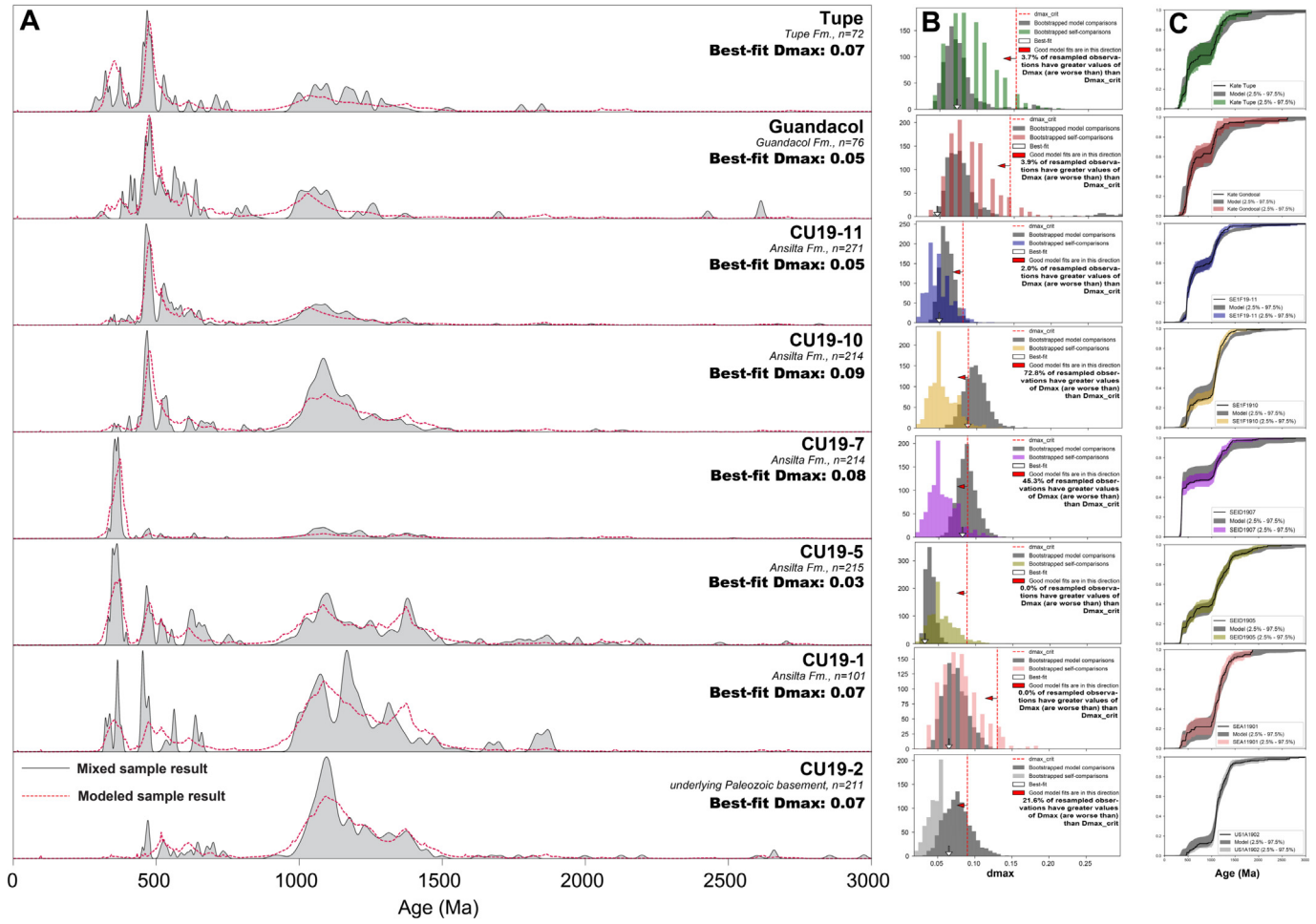

Fig. 7. (A) Probability density plots (black) and Kernel density estimates of the Calingasta-Uspallata and Paganzo basin samples (n = zircons analyzed). The Dmax value (relationship between the actually and modeled cumulative density functions) is indicated. (B) Plot of the distribution of calculated mixing coefficients, or proportions, from each source through the one thousand iterations. (C) Results of the forward mixture modelling. Each plot shows the U–Pb cumulative distributions.

364 Ma, and secondary Mesoproterozoic age modes at 1102 Ma and 1384 Ma. Sample CU19-7 (n = 214; 325 m from base) comes from an interval of sandstone and pebble conglomerate within the diamictite-bearing interval near the top of sequence 4. This sample has a principal age peak of 366 Ma, a lesser peak at 1098 Ma, and the detrital zircon age spectrum ranges from 330 Ma to 2785 Ma. Sample CU19-10 (n = 214; 590 m from base) was collected from a coarsening upward succession of sandstone and conglomerate in sequence 7 of the upper succession (Fig. 3). The detrital zircon age spectrum for this sample ranges from 2129 Ma to 353 Ma and has a detrital zircon age mode of 467 Ma with secondary modes at 537 Ma and 1090 Ma. Sample CU19-11 (n = 271; 695 m from base) was collected from fluvial sandstones from sequence 10 (Fig. 3). The detrital zircon age spectrum of this sample ranges from 3412 Ma to 327 Ma and has a primary detrital zircon age mode of 465 Ma, with secondary age modes of 526 Ma and 1094 Ma. The maximum depositional age for the Ansilta Formation is 332.1 ± 2.2 Ma based on the sampled four youngest zircons with overlapping ages (Fig. 8).

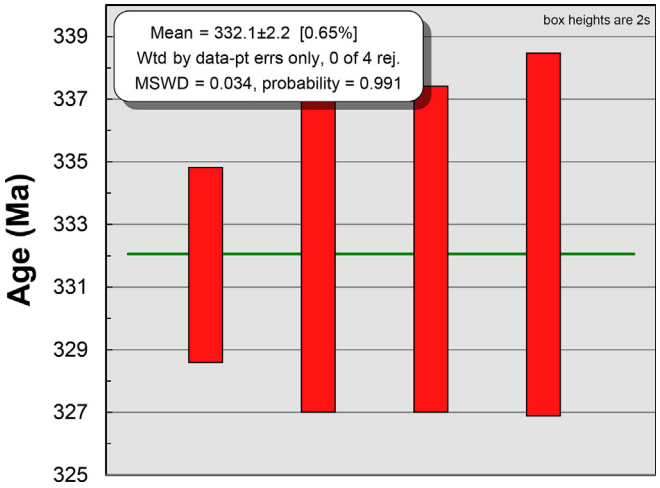

Fig. 8. Maximum depositional age of the Ansilta Formation as determined from the youngest subset of grains with overlapping ages.

4.2. Multidimensional scaling

The source area composite detrital zircon age spectra reveals four distinct data clusters in 3-D MDS space (Fig. 9). The first cluster includes the three Precordillera and western Sierras Pampeanas composites. The Rio de la Plata Craton and eastern Sierras Pampeanas form a second cluster. The Famatinian Belt and Late Paleozoic accretionary complex form a third cluster, and the Carboniferous arc composites form the fourth.

Multidimensional scaling reveals a tight clustering of the three Precordillera and the western Sierras Pampeanas source areas. This

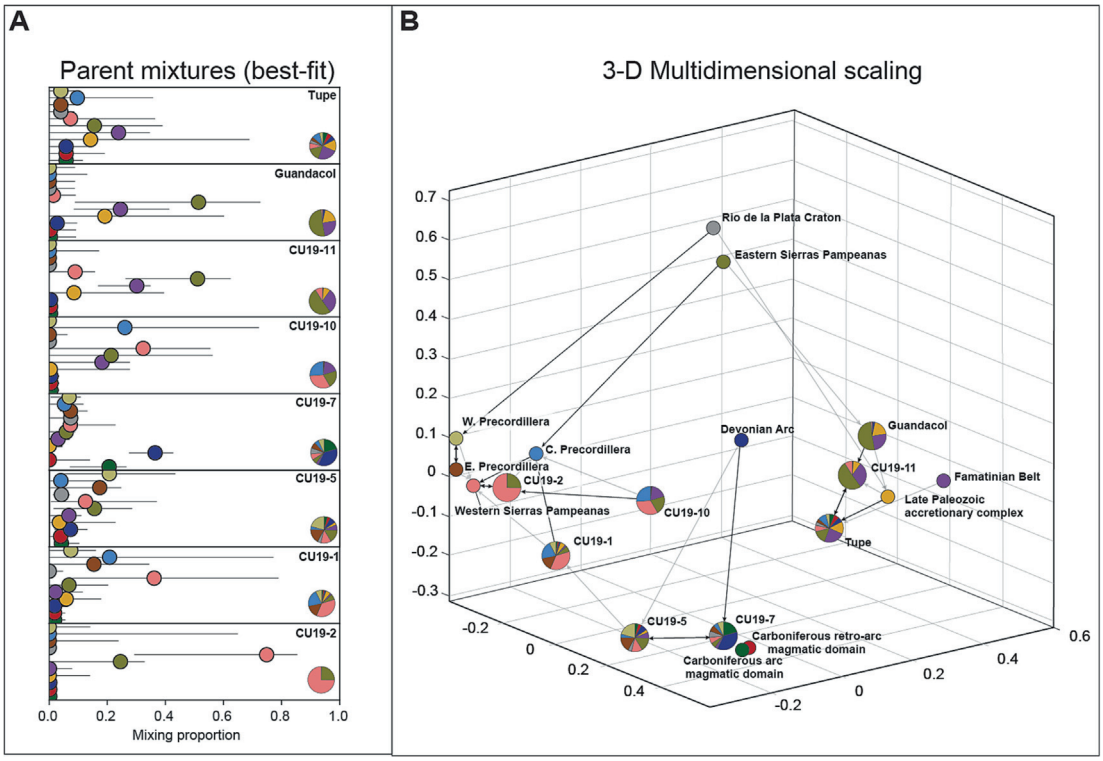

Fig. 9. (A) Plot of relative source contributions (phi) for the Ansilta Formation samples. Circles denote the best fit mixtures, while pie charts depict the total best fit proportions. (B) Three-dimensional multidimensional scaling (MDS) comparisons of detrital zircon U–Pb ages. Parent source terranes are indicated by the smaller variably colored circles. The pie charts are the various Ansilta samples. Heavy arrows indicate closest comparison. Light arrows indicate second closest comparison. Age proportion colors are indicated in Fig. 5.

cluster also includes our sample CU19-2, which we collected from immediately below the sub-Ansilta unconformity from the Ordovician basement. Sample CU19-1 from the base of the Ansilta also plots within this cluster and is a K-S match with CU19-2. Sample CU19-5, according to the K-S analysis, is statistically indistinguishable from CU19-1 and thus also has a strong affinity for the Protoprecordillera source areas. Sample CU19-7 is distinguishable from all the other Ansilta samples, and clusters with the two Carboniferous magmatic arc source composites. Sample CU19-10 is from the upper post-glacial succession. In terms of both K-S and MDS it is distinguishable from everything and looks to be a complicated mixture of clusters 1, 3, and 4. Sample CU19-11 clusters with the Famatinian Belt and the Late Paleozoic accretionary complex and is the closest sample to the Rio de la Plata and Eastern Sierras Pampeanas clusters, all of which are the most distal sediment source areas. The Tupe and Guandacol samples from the Paganzo Basin are part of this cluster as well, and K-S analysis indicates that these age spectra and that of CU19-11 are statistically indistinguishable.

4.3. Source terrane characterization

The Rio de la Plata craton is the southernmost craton in South America; it accreted to Gondwana during the Neoproterozoic-Cambrian. It is located ~ 650 km east of the Sierra Pampeanas and Protoprecordillera and consists mainly of Paleoproterozoic (2.25–2.00 Ga) juvenile crust and a variety of Archean metasedimentary, metavolcanic, and plutonic rocks (Hartmann et al., 2001; Santos et al., 2003). These rocks are overlain by several km of locally derived Neoproterozoic–Silurian continental margin and cratonic strata (Gaucher et al., 2008).

The Precordillera source area is subdivided into west, central, and east; this region is the most proximal to the Ansilta Formation (Gleason et al., 2007; Abre et al., 2012; Thomas et al., 2015; McKenzie et al., 2016; Arnol et al., 2020). Situated within the Cuyania terrane, the Precordillera consists of Mesoproterozoic basement rocks that are overlain by Cambrian cratonic strata and a thick Ordovician clastic wedge. Crustal shortening associated with the collision of the Chilenia terrane during the late Devonian exhumed the Protoprecordillera, making it a prominent eastern highland throughout the Carboniferous. The western Precordillera is characterized by Mesoproterozoic and Neoproterozoic age signatures (1.3–1.0 Ga), derived from Cuyania terrane basement rocks. The central Precordillera consists of higher proportions of Neoproterozoic–Cambrian age signatures, likely from overlying Neoproterozoic–Cambrian strata (Thomas et al., 2015). The eastern Precordillera displays a noticeable lack of Cambrian–Neoproterozoic ages, however a significant 1.3–1.0 Ga mode is observed.

The Sierras Pampeanas are situated east of the Precordillera and divides the Paganzo Basin. We subdivide the Sierras Pampeanas into eastern and western domains. The western Sierras Pampeanas consist of 1.3–1.0 Ga basement massifs of the Cuyania terrane (Naipauer et al., 2010; Ramacciotti et al., 2015; Rapela et al., 2016) with an overlying Neoproterozoic metasedimentary succession with the same zircon age spectrum. The eastern Sierras Pampeanas exhibit a similar 1.3–1.0 Ga signature. However, this region shows a high proportion of 650–500 Ma U–Pb signatures owing to the presence of Neoproterozoic to Ordovician low–high grade metasedimentary rocks that are intruded by extensive granites of the early Cambrian Pampean orogeny (Schwartz et al., 2008; Rapela et al., 2016).

The Ordovician granitoids of the Famatinian magmatic arc intruded into a thick early Paleozoic metasedimentary succession of the Sierras Pampeanas, providing an Ordovician (~476 Ma) age mode. The accretion of the Cuyania terrane outboard of the

Gondwanan margin later in the Ordovician led to the cessation of arc magmatism (Pankhurst et al., 2000; Ducea et al., 2010). Superimposed upon the Sierras Pampeanas is the middle-late Devonian (Chañic) magmatic arc, characterized by a unimodal zircon age population of ~ 375 Ma (Dahlquist et al., 2013, 2019, 2021; Cámera et al., 2018).

Carboniferous magmatism was interpreted by Dahlquist et al. (2021) to occur in two principal domains: a magmatic arc domain (Dahlquist et al., 2018a, 2018b; Moreno et al., 2020), and a *retro*-arc magmatic domain (Alasino et al., 2012; Fogliata et al., 2012; Dahlquist et al., 2013, 2016, 2018a, 2018b; Cámera et al., 2017; Grande et al., 2021). These two regions display unimodal age populations of 349 Ma and 341 Ma, respectively. While the exact geographic boundaries for these two regions are not well defined, the magmatic domain is more proximal. Magmatic arc domain rocks are also present in the frontal Cordillera, but these were outboard and exposure during Ansilta deposition is doubtful. The *retro*-arc magmatic domain is situated farther eastward within the Sierras Pampeanas system. However, it is also possible that more proximal occurrences of these magmatic rocks of these ages remain to be delineated in the Precordillera.

A late Paleozoic accretionary prism consisting of metasedimentary and metavolcanic rocks occurs within the frontal Cordillera, which was outboard of the Calingasta-Uspallata basin during the deposition of the Ansilta Formation (Hervé et al., 2013). Although most workers invoke an easterly source for Ansilta sediment (Malone et al., 2023a and references therein), recycling from a westerly source cannot be precluded. Thus, we include these data as part of our analysis.

5. Discussion

5.1. Ansilta provenance

The oldest glacially influenced sample (CU19-1) was sourced from Ordovician strata in the Precordillera and western Sierras Pampeanas or recycled from older rocks of the Cuyania basement less than 100 km to the east. Thomas et al. (2015) discuss the provenance of detrital grains from the Middle-Upper Ordovician clastic wedge in the Precordillera, which has detrital zircons from 1350 Ma to 1100 Ma and a secondary mode from 1500 Ma to 1350 Ma. They interpret the strata as having formed as an accretionary prism that derived sediment from the western Sierras Pampeanas (younger Proterozoic-aged population) and a Laurentian source (older ages). Ordovician aged strata located 5–10 km to the east and immediately to the north of our study area indicate that the local basement underlying the Ansilta Formation likely served as the main source for the 1170 Ma and 1078 Ma age grains (Thomas et al., 2015). The Devonian zircons within the sample set for the Ansilta Formation likely originated from granitic complexes in the Andean Frontal Cordillera, Precordillera, or the Famatinian Arch (Dahlquist et al., 2018a,b; Moreno et al., 2020). This restricted, proximal source area supports the interpretation of valley glaciers sourced in a high Protoprecordillera that discharged into a marine setting during early Ansilta Formation deposition (Enkelmann et al., 2014; Craddock et al., 2019; Pauls et al., 2021; Malone et al., 2023a). This also is consistent with recent work by Ives et al. (2022) on LPIA strata in Tasmania that involves a "local first" approach to understanding glacially influenced sedimentary provenances.

Sample CU19-05 also was sourced proximally in the Precordillera or western Sierras Pampeanas but shows an increasing quantity of first-cycle Devonian zircons. This is interpreted to represent deriving sediment directly from a late Devonian to early Carboniferous aged intrusive complex or reworked from an equivalent volcanic deposit. Late Devonian to Early Carboniferous intrusions are not reported in the southern and central Precordillera, however Moreno et al. (2020) and a geologic map of La Rioja Province (Guerrero et al., 1993) show small intrusions of this age in the northern Precordillera in the vicinity of Sierra de la Punilla and Sierra de Maz. In the Cerro Veladéro area, early Carboniferous granites are partially exposed in paleovalley walls underlying the diamictite-bearing Quebrada Larga Formation (Limarino et al., 2014a). These are the closest intrusions of this age to the Ansilta Formation, so it is interpreted that this area could provide the source for the Devonian and would indicate an ice center situated over the northern Precordillera.

Sample CU19-07 is dominated by a Devonian arc age peak, and the absence of significant Famatinian and Mesoproterozoic ages imply that ice was sourcing material from local post-orogenic granitic intrusions during the height of glaciation with minimal sediment reworking. The closest source of late Devonian to early Carboniferous intrusions occur in the northern Precordillera (Dahlquist et al., 2018a,b; Moreno et al., 2020).

Upon closer inspection of the probability density plot, there are two detrital zircon age modes evident at ~ 355 Ma and ~ 366 Ma, respectively. Plutonic rocks of this age occur in the Achala batholith in the eastern Sierras Pampeanas, which is more than 250 km to the east of the study area and across the Paganzo Basin. If these zircons were indeed sourced from the east, this would indicate more extensive glaciation in southwest Gondwana at this time. This would support the interpretation of Starck et al. (2021) of an ice sheet that extended from the Rio de la Plata craton to the northern Precordillera. We do not favor this interpretation, as Moxness et al. (2018) and Pauls et al. (2021) only found direct evidence of glaciation along the western margin of the Paganzo basin, and these deposits were sourced from the Precordillera further to the west. No evidence for glaciation was observed in strata present in the eastern Paganzo Basin, which would be necessary as the Achala batholith occurs east of these deposits. A third hypothesis is that late Devonian–early Carboniferous batholiths exist in the Precordillera itself, and these rocks are either eroded away, or not yet delineated. We favor this hypothesis because zircons from other distal source terranes are not abundant in this sample. It is possible though that there was variation in topography, glaciation, and sedimentation north–south along the Precordillera strike with discreet basins that have unique sedimentary and tectonic settings.

Samples CU19-10 and CU19-11 have much different detrital zircon age spectra than the lowermost Ansilta Formation samples. No Devonian signal is evident with the ~ 465 Ma Famatinian signal being dominant and Pampean (~530 Ma) and Grenville (~1090 Ma) ages being smaller. These signals share some resemblance to the lowermost Ansilta Formation sample (CU19-01) with the distinction of having greater Famatinian age zircon grains in the population, so it is likely that these grains were derived locally from the underlying Ordovician and Silurian aged basement as well as reworked from Carboniferous strata to the east. Sample CU19-11 contained the oldest analyzed zircons, including three that are > 3000 Ma. These likely were derived from the Rio de la Plata craton but may have been recycled multiple times (Hartmann et al., 2001; Santos et al., 2003; Gaucher et al., 2008).

Sample CU19-11 shares detrital zircon age spectrum characteristics with the Tupe and Guandacol formation samples from the Paganzo Basin (Pauls, 2020; Pauls et al., 2021) that support a distal eastern source area for these zircons. We interpret this to support the late Carboniferous collapse of the Protoprecordillera as a sediment barrier for the Ansilta region and source of alpine glaciation to the Paganzo and Calingasta-Uspallata basins. Instead, a connection of the basins by fluvial-marine systems through the formerly glaciated paleovalleys is evident.

The central Cordillera to the west was not a principal source area for the Ansilta Formation. The composite detrital zircon spectrum of Central Cordillera rocks is statistically related to the upper Ansilta, Tupe, and Guandacol and these share a common sediment source. We interpret the late Paleozoic accretionary complex to be the down-slope correlative of the Ansilta Formation.

It is interesting to note that the Rio de la Plata craton was not a principal sediment source for the upper Ansilta Formation as the catchment does not appear to have extended beyond the eastern Sierras Pampeanas and Famatinian regions. This could also be because this region was covered by ice during late Ansilta and Tupe deposition and synchronous with the earliest phases of Late Pennsylvanian–Early Permian glaciation in eastern South America.

5.2. Timing of Ansilta Formation deposition

. The maximum depositional age of ~ 330 Ma suggests that the Ansilta Formation is broadly coeval with similar strata in the Calingasta-Uspallata Basin as well as in the Río Blanco and Paganzo basins (i.e. Río del Peñon, Tupe, and Guandacol formations) and was likely deposited during and after the Serpukhovian-Bashkirian glacial episode (Limarino et al., 2006, 2014; Henry et al., 2010; López-Gamundi and Buatois, 2010; Isbell et al., 2012, 2021; Montañez and Poulsen, 2013; Craddock et al., 2019; López-Gamundí et al., 2021). Gulbranson et al. (2010) delineated a ~ 320 Ma ash bed in the basal transgressive succession of the Río del Peñon (Guandacol equivalent) in the Río Blanco Basin that marks the lower age limit of the Serpukhovian-Bashkirian glacial episode there. We believe this to be a reasonable age estimate for the termination of glaciation in the lower Ansilta Formation as the Calingasta-Uspallata and the Río Blanco basins are N–S contiguous features. Although ample evidence for the earlier Visean glaciation exists elsewhere in southwest Gondwana (e.g., Caputo and Crowell, 1985; Caputo et al., 2008; Rocha-Campos et al., 2008; Gulbranson et al., 2010), the upper limit of ~ 335 Ma for this episode is too old to be recorded in the Ansilta Formation.

The youngest Ansilta Formation zircons are unlikely to have originated from Carboniferous intrusions. Instead, these grains may have been derived from the active magmatic arc situated along the Panthalassa margin offboard to the west (Hervé et al., 2013). It is also admissible that sequences 9–10 are latest Pennsylvanian or earliest Permian in age, as would be consistent with the biostratigraphic work of Césari et al. (2014). Our data also indicates that the Protoprecordillera collapse occurred no earlier than the end of the Bashkirian (~315 Ma) at this location. This contrasts with the ideas proposed by Milana and Di Pasquo (2023) for correlative strata to the north, that the Precordillera was not a significant topographic barrier at any time after the late Devonian.

5.3. Late Carboniferous collapse of the Precordillera

The Precordillera region of Western Argentina has taken on importance in determining the extent of LPIA glaciation in western Gondwana. One hypothesis suggests the occurrence of an extensive ice sheet extending over eastern South America (Milana and Bercowski, 1993; Aquino et al., 2014; Valdez Buso et al., 2021; Milana and Di Pasquo, 2023) from an ice center located over either the Rio de la Plata Craton in eastern South America, southern Africa, or in Antarctica (Scotese and Barrett, 1990; Starck and del Papa, 2006; Starck et al., 2021). In this scenario, outlet glaciers dissected a low lying hummocky coastal area in the Precordillera region drained ice from this eastern ice sheet into marine embayments to the west (Valdez Buso et al., 2017, 2021; Milana and Di Pasquo, 2019, 2023).

The other hypothesis suggests that a number of ice centers and alpine/valley glaciers formed on uplands in western Argentina

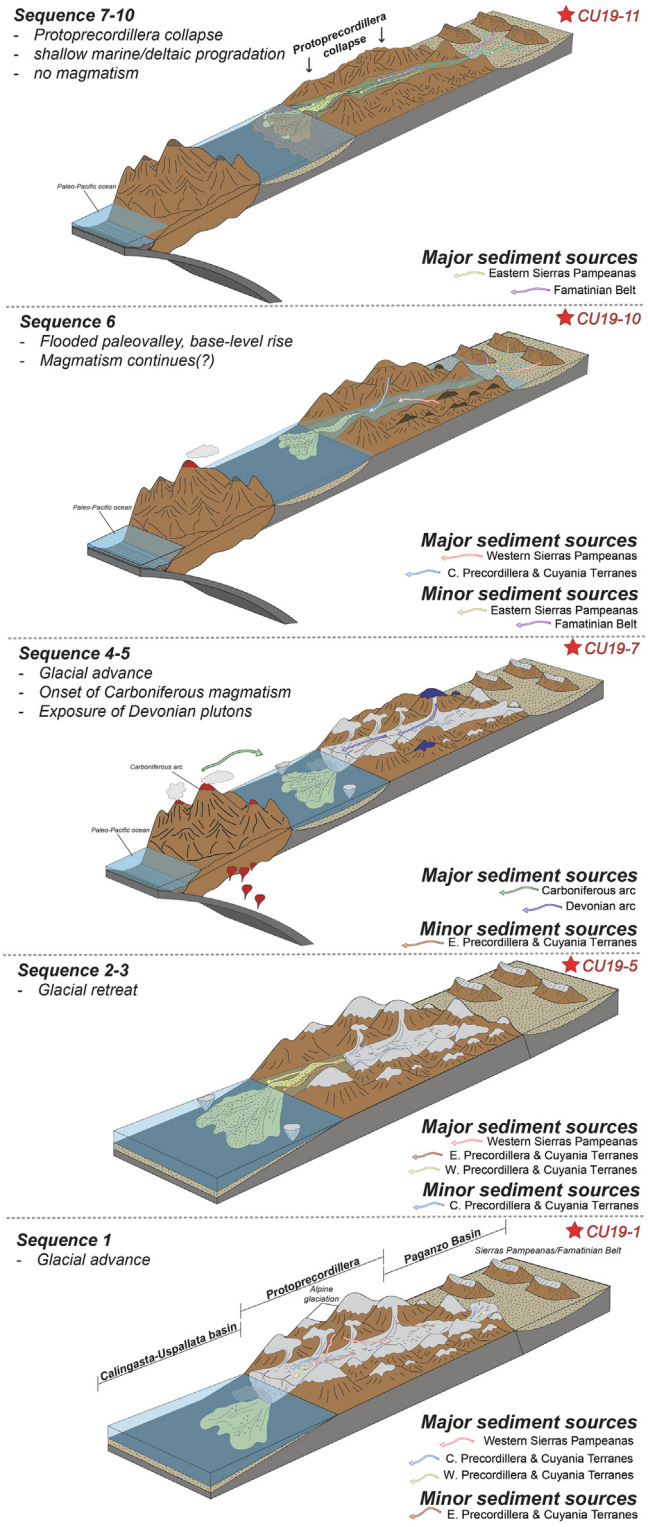

Fig. 10. Reconstruction of Ansilta Deposition in the Calingasta-Upsalatta basin. Beginning of Episode II Glaciation (sequences 1–3; samples CU19-1 and CU 19–5): Glacially influenced forearc basin adjacent to a high Precordillera with locally derived sediment. Culmination of Episode II Glaciation (sequence 4–5; CU19-7): Glacially influenced intra-arc basin. The appearance of late Devonian and early Carboniferous zircons indicate the erosional denudation and tectonic collapse of the Precordillera caused by the outward shift in subduction and development of arc magmatism in the main Cordillera. Sediment remains locally derived. Flooding of the Ansilta paleovalley (sequence 6; sample CU19-10): Post-glacial mudstone sedimentation replaces diamictites following the demise of local glaciation. Post Episode II Glaciation (sequence 7–10; sample CU19-11): Precordillera collapse causes the end of alpine glaciation. The upper Ansilta formed in a *retro*-arc basin with sediment derived from distal sources in the Famatinian belt and Sierras Pampeanas. Sediment is transported through a system of paleovalleys that connect through the Paganzo Basin.

including a substantial discontinuous upland, the Protoprecordillera, from which, valley glaciers/fjords radiated outward away from highs (López-Gamundí et al., 1994; Henry et al., 2008; Limarino et al., 2014a), flowing towards the N, S, E, and W (e.g., Scalabrini Ortiz, 1972; Andreis et al., 1975; Buatois and Mángano, 1994; López-Gamundí et al., 1994, 2016; López-Gamundí and Martınez, 2000, 2003; Kneller et al., 2004; Marenssi et al., 2005; Dykstra et al., 2006; Henry et al., 2008, 2010; Aquino et al., 2014; Limarino et al., 2014a; Malone et al., 2023a; Milana and Di Pasquo, 2023). Valleys cutting into these uplands were at least 1000 m deep (top of the valley walls to basal deltaic deposits; cf. Dykstra et al., 2006). Limarino et al. (2014a), Pauls et al. (2019), Pauls (2020) and Correa et al. (2022) suggested that the Protoprecordillera formed a partial barrier to circulation of moisture (orographic effect) and marine waters from the Panthallasan margin during glacial times. Post glacial connections between the east and west were established either by breaching of barriers, or by collapse of the Protoprecordillera during late Bashkirian time (Limarino et al., 2014a; Correa et al., 2022).

The identification of sediment routing patterns during the mid Carboniferous glaciation in the Precordilleran region of Argentina is critical in determining the paleogrography of western Gondwana and determining ice extent during the LPIA. Results of our work indicate that glaciogenic deposits were sourced locally from rocks exposed in the current Precordilleran and that sediment was not derived from an ice sheet centered over eastern South America (Fig. 10). There was little to no connection between Ansilta strata and strata currently exposed in the Paganzo Basin. Distal sources in the Sierra Pampeanas and the Rio de la Plata Craton occur during development of post-glacial, shallow marine and fluvial deltaic sedimentation in the Ansilta Formation suggesting that either the upland housing the earlier glaciers was breached or that the Protoprecordillera collapsed allowing sediment from the east into the Calingasta-Uspallata Basin.

6. Conclusions

The following conclusions can be drawn from this research:

(1) The detrital zircon grains of the glacially influenced lower Ansilta Formation were sourced locally in the Protoprecordillera. Alpine glaciers filled paleovalleys and discharged directly to the sea. This indicates that the Precordillera was high and humid enough to seed glaciers. Moreover, both ice and Precordillera bedrock served as barriers for distally derived sediment. This contrasts with the ideas proposed by Milana and Di Pasquo (2023) for correlative strata to the north, that the Precordillera was not a significant topographic barrier after the late Devonian.

(2) The non-glacial upper Ansilta Formation was sourced in the Sierras Pampeanas and Famatinian terranes. This occurred following the collapse of the Protoprecordillera and represents that a drainage link occurred between the Calingasta-Uspallata and Paganzo basins during the late Pennsylvanian-Cisuralian.

CRediT authorship contribution statement

Joshua R. Malone: Visualization, Investigation, Conceptualization, Methodology, Formal analysis, Data curation, Software, Resources, Writing - original draft, Writing - review & editing. **John E. Malone:** Conceptualization, Investigation, Writing - review & editing, Resources, Supervision. **John L. Isbell:** Investigation, Writing - review & editing, Supervision, Resources, Project administration, Funding acquisition. **David H. Malone:** Conceptualization, Investigation, Writing - review & editing. **John P. Craddock:** Writing - review & editing, Funding acquisition. **Kate N. Pauls:** Writing - review & editing, Funding acquisition.

Declaration of competing interest

The authors declare that they have no known competing financial interests or personal relationships that could have appeared to influence the work reported in this paper.

Acknowledgements

Financial support for this study was provided by grants from the USA's National Science Foundation (Grant Nos. 1443557, 1559231, and 1729219). A special thank you to Glen Sharman and Sam Johnstone for providing access to the detritalPy-mix code. We thank George Gehrels, Mark Pecha, and staff at the Arizona Laserchron Center (ALC) for assistance with obtaining U–Pb detrital zircon data as well as NSF-EAR 1649254 for support of the ALC. We thank Milo Barham and an anonymous reviewer for their thoughtful reviews that improved this manuscript.

Appendix A. Supplementary data

Supplementary data to this article can be found online at https://doi.org/10.1016/j.gsf.2024.101807.

References

Abre, P., Cingolani, C.A., Cairncross, B., Chemale Jr, F., 2012. Siliciclastic Ordovician to Silurian units of the Argentine Precordillera: Constraints on provenance and tectonic setting in the proto-Andean margin of Gondwana. J. S. Am. Earth Sci. 40, 1–22.

Alasino, P.H., Dahlquist, J.A., Pankhurst, R.J., Galindo, C., Casquet, C., Rapela, C.W., Larrovere, M.A., Fanning, C.M., 2012. Early Carboniferous sub-to mid-alkaline magmatism in the Eastern Sierras Pampeanas, NW Argentina: A record of crustal growth by the incorporation of mantle-derived material in an extensional setting. Gondw. Res. 22, 992–1008.

Alonso-Muruaga, P.J., Limarino, C.O., Spalletti, L.A., Colombo Piñol, F., 2018. Depositional settings and evolution of a fjord system during the carboniferous glaciation in Northwest Argentina. Sed. Geol. 369, 28–45.

Amos, A.J., López-Gamundí, O.R., 1981. Late Paleozoic tillites and diamictites of the Calingasta-Uspallata and Paganzo basins, western Argentina. Earth's Pre-Pleistocene Glacial Record, 859–868.

Amos, A.J., Rolleri, E., 1965. El Carbónico marino en el valle Calingasta-Uspallata, San Juan-Mendoza. Boletin De Informaciones Petroleras 368, 50–71 (in Spanish).

An, X., Huan, X., He, K., Xia, L., Du, Y., Ding, J., Yuan, T., Liu, G.-Z., Zheng, H., 2023. Onset of the late Paleozoic glaciation in the Lhasa terrane. Southern Tibet. Global Planet. Change 225, 104139.

Andreis, R.R., Mazzoni, M.M., Spalletti, L.A., 1975. Estudio estratigráfico y paleoambiental de las sedimentitas terciarias entre Pico Salamanca y Bahía Bustamante, Provincia de Chubut, República Argentina. Rev. Asoc. Geol. Argent. 30, 1 (in Spanish).

Aquino, C.D., Milana, J.P., Faccini, U.F., 2014. New glacial evidences at the Talacasto paleofjord (Paganzo basin, W-Argentina) and its implications for the paleogeography of the Gondwana margin. J. S. Am. Earth Sci. 56, 278–300.

Ariza, J.P., Boedo, F.L., Sánchez, M.A., Christiansen, R., Lujan, S.B.P., Vujovich, G.I., Martínez, P., 2018. Structural setting of the Chanic orogen (Upper Devonian) at central-western Argentina from remote sensing and aeromagnetic data. Implications in the evolution of the proto-Pacific margin of Gondwana. J. S. Am. Earth Sci. 88, 352–366.

Arnol, J.A., Uriz, N.J., Cingolani, C.A., Basei, M.A.S., Abre, P., 2020. Provenance analysis of Devonian peripheral foreland basins in SW Gondwana, case of the Gualilán Group. Precordillera Argentina. Int. J. Earth Sci. 109, 2467–2494.

Arnol, J.A., Uriz, N.J., Cingolani, C.A., Abre, P., Basei, M.A.S., 2022. Provenance evolution of the San Juan Precordillera Silurian-Devonian basin (Argentina): Linking with other depocentres in Cuyania terrane. J. S. Am. Earth Sci. 115, 103766.

Buatois, L.A., Mángano, M.G., 1994. Lithofacies and depositional processes from a Carboniferous lake, Sierra de Narváez, northwest Argentina. Sed. Geol. 93, 25–49.

Cagliari, J., Philipp, R.P., Buso, V.V., Netto, R.G., Klaus Hillebrand, P., da Cunha Lopes, R., Stipp Basei, M.A., Faccini, U.F., 2016. Age constraints of the glaciation in the Parana Basin; evidence from new U-Pb dates. J. Geol. Soc. 173, 871–874.

Cagliari, J., Schmitz, M.D., Tedesco, J., Trentin, F.A., Lavina, E.L.C., 2023. High-precision U-Pb geochronology and Bayesian 1 age-depth modeling of the glacial-postglacial transition of the southern Paraná Basin: detailing the terminal phase of the Late Paleozoic Ice Age on Gondwana. Sediment. Geol. 451, 106397.

Cámera, M.M.M., Dahlquist, J.A., Basei, M.A., Galindo, C., Neto, M.D.C.C., Facetti, N., 2017. F-rich strongly peraluminous A-type magmatism in the pre-Andean

foreland Sierras Pampeanas, Argentina: Geochemical, geochronological, isotopic constraints and petrogenesis. Lithos 277, 210–227.
Cámera, M.M.M., Dahlquist, J.A., Ramacciotti, C.D., Galindo, C., Basei, M.A., Zandomeni, P.S., Grande, M.M., 2018. The strongly peraluminous A-type granites of the Characato suite (Achala batholith), Sierras Pampeanas, Argentina: Evidence of Devonian-Carboniferous crustal reworking. J. S. Am. Earth Sci. 88, 551–567.
Caputo, M.V., Crowell, J.C., 1985. Migration of glacial centers across Gondwana during Paleozoic Era. Geol. Soc. Am. Bull. 96, 1020–1036.
Caputo, M.V., de Melo, J.H.G., Streel, M., Isbell, J.L., Fielding, C.R., 2008. Late Devonian and early Carboniferous glacial records of South America. Geol. Soc. Am. Spec. Pap. 441, 161–173.
Caputo, M.V., dos Santos, R.O.B., 2020. Stratigraphy and ages of four Early Silurian through Late Devonian, Early and Middle Mississippian glaciation events in the Parnaíba Basin and adjacent areas, NE Brazil. Earth-Sci. Rev. 207, 103002.
Casquet, C., Baldo, E., Pankhurst, R.J., Rapela, C.W., Galindo, C., Fanning, C.M., Saavedra, J., 2001. Involvement of the Argentine Precordillera Terrane in the Famatinian mobile belt: Geochronological (U–Pb SHRIMP) and metamorphic evidence from the Sierra de Pie de Palo. Geology 29, 703–706.
Casquet, C., Rapela, C.W., Pankhurst, R.J., Baldo, E.G., Galindo, C., Fanning, C.M., Dahlquist, J.A., Saavedra, J., 2012. A history of Proterozoic terranes in southern South America: from Rodinia to Gondwana. Geosci. Front. 3, 137–145.
Césari, S.N., Gutiérrez, P.R., 2001. Palynostratigraphy of upper Paleozoic sequences in central-western Argentina. Palynology 24, 113–146.
Césari, S.N., Gaido, M.F., Cegarra, M.I., Anselmi, G., 2014. The first record of Permian flora in the Ansilta Formation (Western Precordillera of Argentina) and its regional correlation. Ameghiniana 51, 428–432.
Césari, S.N., Limarino, C.O., Spalletti, L.A., Piñol, F.C., Perez Loinaze, V.S., Ciccioli, P.L., Friedmane, R., 2019. New U-Pb zircon age for the Pennsylvanian in Argentina: Implications in palynostratigraphy and regional stratigraphy. J. S. Am. Earth Sci. 92, 400–416.
Césari, S.N., Perez Loinaze, V.S., 2021. Update of the Pennsylvanian palynostratigraphy from central-western Argentina. J. S. Am. Earth Sci. 106, 102933.
Césari, S.N., Limarino, C.O., Gulbranson, E.L., 2011. An upper Paleozoic bio-chronostratigraphic scheme for the western margin of Gondwana. Earth Sci. Rev. 106, 149–160.
Choudhuri, A., Mandal, S., Bumby, A., Pillai, S., 2023. Glacial sedimentation in Northern Gondwana: Insights from the Talchir formation, Manendragarh. India. Geol. Mag. 160, 1228–1240.
Columbi, C.E., Limarino, C.O., Césari, S.N., 2018. La sucesión Carbonífera de la Quebrada Aguade la Peña (Sierra de Valle Fértil): Ambientes sedimentarios, contenido fosilífero eimportancia estratigráfica. Latin American Journal of Sedimentology and Basin Analysis 25, 19–53.
Correa, G., Drovandi, J., Taboada, A., Colombi, C., Conde, O., 2022. The collapse of the Protoprecordillera and unification of the Paganzo and Calingasta-Uspallata basins: Retamito Formation a key in the integrative biostratigraphic and palaeoenvironmental model. J. S. Am. Earth Sci. 119, 103997.
Craddock, J.P., Ojakangas, R.W., Malone, D.H., Konstantinou, A., Mory, A., Bauer, W., Thomas, R.J., Craddock-Affinati, S., Pauls, K., Zimmerman, U., Botha, G., Rochas-Campos, A., Tohver, E., Riccomini, C., Martin, J., Redfern, J., Horstwood, M., Gehrels, G., 2019. Provenance of Permo-Carboniferous glacial diamictites across Gondwana. Earth Sci. Rev. 192, 285–316.
Crowell, J.C., 1999. Pre-Mesozoic Ice Ages: Their bearing on understanding the climate system. Geol. Soc. Am. Mem., p. 192.
Crowell, J.C., Frakes, L.A., 1970. Phanerozoic glaciation and the causes of ice ages. Am. J. Sci. 268, 193–224.
Csaky, A., 1963. Geología de la zona situada al norte del Cordón del Naranjo y al sur del Cerro Las Cabeceras, departamento Calingasta provincia de San Juan. Facultad De Ciencias Extractas y Naturales De La Universidad Nacional De Buenos Aires (in Spanish).
Dahlquist, J.A., Alasino, P.H., Nelson Eby, G., Galindo, C., Casquet, C., 2010. Fault controlled Carboniferous A-type magmatism in the proto-Andean foreland (Sierras Pampeanas, Argentina): geochemical constraints and petrogenesis. Lithos 115, 65–81.
Dahlquist, J.A., Pankhurst, R.J., Gaschnig, R.M., Rapela, C.W., Casquet, C., Alasino, P. H., Galindo, C., Baldo, E.G., 2013. Hf and Nd isotopes in Early Ordovician to Early Carboniferous granites as monitors of crustal growth in the Proto-Andean margin of Gondwana. Gondw. Res. 23, 1617–1630.
Dahlquist, J.A., Verdecchia, S.O., Baldo, E.G., Basei, M.A., Alasino, P.H., Urán, G.A., Rapela, C.W., Costa Campos Neto, M.D., Zandomeni, P.S., 2016. Early Cambrian U-Pb zircon age and Hf-isotope data from the Guasayán pluton, Sierras Pampeanas, Argentina: implications for the northwestern boundary of the Pampean arc. Andean Geol. 43, 137–150.
Dahlquist, J.A., Alasino, P.H., Basei, M.A., Cámera, M.M.M., Grande, M.S.M., Neto, M. D.C.C., Larrecharte, M.G., 2018a. Recurrent intrusive episodes in the Paleozoic metasedimentary upper crust during the Early Carboniferous time: The Veladero granitoid stock and the peraluminous andesite. J. S. Am. Earth Sci. 88, 80–93.
Dahlquist, J.A., Alasino, P.H., Basei, M.A., Cámera, M.M.M., Grande, M.M., Neto, M.D. C.C., 2018b. Petrological, geochemical, isotopic, and geochronological constraints for the Late Devonian-Early Carboniferous magmatism in SW Gondwana (27–32 LS): an example of geodynamic switching. Int. J. Earth Sci. 107, 2575–2603.
Dahlquist, J.A., Grande, M.M., Alasino, P.H., Basei, M.A., Galindo, C., Moreno, J.A., Cámera, M.M.M., 2019. New geochronological and isotope data for the Las Chacras-Potrerillos and Renca batholiths: a contribution to the Middle-Upper Devonian magmatism in the pre-Andean foreland (Sierras Pampeanas, Argentina), SW Gondwana. J. S. Am. Earth Sci. 93, 48–363.
Dahlquist, J.A., Cámera, M.M.M., Alasino, P.H., Pankhurst, R.J., Basei, M.A., Rapela, C. W., Moreno, J.A., Baldo, E.G., Galindo, C., 2021. A review of Devonian-Carboniferous magmatism in the central region of Argentina, pre-Andean margin of SW Gondwana. Earth Sci. Rev. 221, 103781.
Dahlquist, J.A., Morales Camera, M.M., Alasino, P.H., Tickyj, H., Basei, M.A., Galindo, C., Moreno, J.A., Rocher, S., 2022. Geochronology and geochemistry of Devonian magmatism in the Frontal cordillera (Argentina): geodynamic implications for the pre-Andean SW Gondwana margin. Int. Geol. Rev. 64, 233–253.
Dávila, F.M., Martina, F., Parra, M., Ávila, P., 2021. Effects of uplift on Carboniferous exhumation and mountain glaciations in Pericratonic Areas of SW Gondwana, Central Argentina. Tectonics 40, (12) e2021TC006855.
De Rosa, L., 1983. Sedimentitas continentales del Carbónico inferior en el flanco occidental de la Precordillera, departamento Calingasta, provincia de San Juan. Revista De La Asociación Argentina De Mineralogía, Petrografía y Sedimentología 14, 51–69 (in Spanish).
Díaz-Martínez, E., Vavrdová, M., Bek, J., Isaacson, P.E., 1999. Late Devonian (Famennian) glaciation in western Gondwana: evidence from the Central Andes. Abhandlungen Der Geologischen Bundesanstalt 54, 213–238.
Ducea, M.N., Otamendi, J.E., Bergantz, G., Stair, K.M., Valencia, V.A., Gehrels, G.E., 2010. Timing constraints on building an intermediate plutonic arc crustal section: U-Pb zircon geochronology of the Sierra Valle Fértil–La Huerta, Famatinian Arc, Argentina. Tectonics 29 (4), TC4002.
Ducea, M.N., Otamendi, J.E., Bergantz, G.W., Jianu, D., Petrescu, L., 2015. The origin and petrologic evolution of the Ordovician Famatinian-Puna arc. Geol. Soc. Am. Mem. 212, 125–138.
Dykstra, M., Kneller, B., Milana, J.P., 2006. Deglacial and postglacial sedimentary architecture in a deeply incised paleovalley-paleofjord; the Pennsylvanian (Late Carboniferous) Jejenes Formation, San Juan. Argentina. Geol. Soc. Am. Bull. 118, 913–937.
Enkelmann, E., Ridgway, K.D., Carignano, C., Linnemann, U., 2014. A thermochronometric view into an ancient landscape: tectonic setting, and inversion of the Paleozoic eastern Paganzo basin, Argentina. Lithosphere 6, 93–107.
Fielding, C.R., Frank, T.D., Isbell, J.L., 2008a. The late Paleozoic ice age – a review of current understanding and synthesis of global climate patterns. Geol. Soc. Am. Spec. Pap. 441, 343–354.
Fielding, C.R., Frank, T.D., Birgenheier, L.P., Rygel, M.C., Jones, A.T., Roberts, J., 2008b. Stratigraphic imprint of the late Paleozoic ice age in eastern Australia: a record of alternating glacial and nonglacial climate regime. J. Geol. Soc. London 165, 129–140.
Fielding, C.R., Frank, T.D., Birgenheier, L.P., 2022. A revised, late Paleozoic glacial time-space framework for eastern Australia, and comparisons with other regions and events. Earth Sci. Rev. 236, 104263.
Fogliata, A.S., Báez, M.A., Hagemann, S.G., Santos, J.O., Sardi, F., 2012. Post-orogenic, carboniferous granite-hosted Sn–W mineralization in the Sierras Pampeanas Orogen. Northwestern Argentina. Ore Geol. Rev. 45, 16–32.
Freiburg, J.T., Malone, D.H., Huisman, M., 2022. Geochronology of Cambrian Sedimentary and Volcanic Rocks in the Illinois Basin: Defining the Illinois Aulacogen. The Sedimentary Record. pp. 1–11.
García-Sansegundo, J., Farias, P., Rubio-Ordóñez, Á., Clariana, P., Cingolani, C., Heredia, N., 2023. Polyorogenic structure of the San Rafael Block, Mendoza, Argentina: New data for the interpretation of the Chanic Orogen. J. S. Am. Earth Sci. 124, 104277.
Gaucher, C., Finney, S.C., Poiré, D.G., Valencia, V.A., Grove, M., Blanco, G., Pamoukaghlián, K., Peral, L.G., 2008. Detrital zircon ages of Neoproterozoic sedimentary successions in Uruguay and Argentina: insights into the geological evolution of the Río de la Plata Craton. Precambr. Res. 167, 150–170.
Gehrels, G.E., Valencia, V., Pullen, A., 2006. Detrital zircon geochronology by Laser-Ablation Multicollector ICPMS at the Arizona LaserChron Center. In: Loszewski, T., Huff, W. (Eds.), Geochronology: Emerging Opportunities, Paleontology Society Short Course. Paleontology Society Papers, 11, 1-10.
Gehrels, G., Pecha, M., 2014. Detrital zircon U-Pb geochronology and Hf isotope geochemistry of Paleozoic and Triassic passive margin strata of western North America. Geosphere 10, 49–65.
Gehrels, G.E., Valencia, V., Ruiz, J., 2008. Enhanced precision, accuracy, efficiency, and spatial resolution of U-Pb ages by laser ablation-multicollector-inductively coupled plasma-mass spectrometry. Geochem. Geophys. Geosyst. 9 (3), Q03017.
Gleason, J.D., Finney, S.C., Peralta, S.H., Gehrels, G.E., Marsaglia, K.M., 2007. Zircon and whole-rock Nd-Pb isotopic provenance of Middle and Upper Ordovician siliciclastic rocks, Argentine Precordillera. Sedimentology 54, 107–136.
Gómez Tapias, J., Schobbenhaus, C., Montes Ramírez, N., 2019. Geological Map of South America 2019.
Grande, M.M., Alasino, P., Dahlquist, J., Cámera, M.M., Galindo, C., Basei, M., 2021. Thermal maturation of a complete magmatic plumbing system at the Sierra de Velasco, Northwestern Argentina. Geol. Mag. 158, 537–554.
Griffis, N.P., Mundil, R., Montanez, I.P., Isbell, I., Fedorchuk, N., Vesely, F., Iannuzzi, R., Yin, Q.Z., 2018. A new stratigraphic framework built on U-Pb single zircon TIMS ages and implications for the timing of the penultimate icehouse (Paraná Basin, Brazil). Geol. Soc. Am. Bull. 130, 848–858.
Griffis, N.P., Montañez, I.P., Mundil, R., Richey, J., Isbell, J., Fedorchuk, N., Linol, B., Iannuzzi, R., Vesely, F., Mottin, T., da Rosa, E., Keller, B., Yin, Q.-Z., 2019. Coupled

stratigraphic and U-Pb zircon age constraints on the late Paleozoic icehouse-to-greenhouse turnover in south-central Gondwana. Geology 47, 1146–1150.
Guerrero, M.A., Lavandaio, E., Marcos, O., 1993. Mapa Geologico de la Provincia de la Rioja, Republica Argentina. Secretaria De Mineria Direccion Nacional Del Servicio Geologico, Escala 1:500,000 (in Spanish).
Gulbranson, E.L., Montanez, I.P., Schmitz, M.D., Limarino, C.O., Isbell, J.L., Marenssi, S.A., Crowley, J.L., 2010. High-precision U-Pb calibration of Carboniferous glaciation and climate history, Paganzo Group, NW Argentina. Geol. Soc. Am. Bull. 122, 1480–1498.
Harrington, H.J., 1971. Descripción geológica de la Hoja ramblón 22c, provincias de Mendoza y San Juan. Boletín Dirección Nacional De Geología y Minería 114, 7–87 (in Spanish).
Hartmann, L.A., Campal, N., Santos, J.O.S., McNaughton, N.J., Bossi, J., Schipilov, A., Lafon, J.M., 2001. Archean crust in the Rio de la Plata Craton, Uruguay-SHRIMP U-Pb zircon reconnaissance geochronology. J. S. Am. Earth Sci. 14, 557–570.
Heckel, P.H., 2008. Pennsylvanian cyclothems in midcontinent North America as far-field effects of waxing and waning of Gondwana ice sheets. Geol. Soc. Am. Spec. Pap. 441, 275–289.
Heckel, P., 2022. North American Midcontinent Pennsylvanian Cyclothems and their implications. Geol. Soc. London Spec. Pub., p. 535.
Henry, L.C., Isbell, J.L., Limarino, C.O., 2008. Carboniferous glaciogenic deposits of the proto-Precordillera of west-central Argentina. Geol. Soc. Am. Spec. Pap. 441, 131–142.
Henry, L.C., Isbell, J.L., Limarino, C.O., McHenry, L.J., Fraiser, M.L., 2010. Mid-Carboniferous deglaciation of the Protoprecordillera, Argentina recorded in the Agua de Jagüel palaeovalley. Palaeogeogr. Palaeoclimatol. Palaeoecol. 298, 112–129.
Hervé, F., Calderón, M., Fanning, C.M., Pankhurst, R.J., Godoy, E., 2013. Provenance variations in the Late Paleozoic accretionary complex of central Chile as indicated by detrital zircons. Gondw. Res. 23, 1122–1135.
Horan, K., Stone, P., Crowhurst, S.J., 2019. Sedimentary record of Early Permian deglaciation in southern Gondwana from the Falkland Islands. Geol. Soc. London Spec. Pub. 475, 131–147.
Huff, W.D., Davis, D., Bergstrom, S.M., Krekeler, M.P.S., Kolata, D.R., Cingolani, C.A., 1998. A biostratigraphically well-constrained K-bentonite U-Pb zircon age of the lowermost Darriwillian Stage (Middle Ordovician) from the Argentine Precordillera. Episodes 20, 29–33.
Isaacson, P.E., Díaz-Martínez, E., Grader, G.W., Kalvoda, J., Bábek, O., Devuyst, F.X., 2008. Late Devonian–earliest Mississippian glaciation in Gondwanaland and its biogeographic consequences. Paleogeography, Paleoclimatology, Paleoecology 268, 126–142.
Isbell, J.L., Miller, M.F., Wolfe, K.L., Lenaker, P.A., 2003. Timing of late Paleozoic Glaciation in Gondwana: was glaciation responsible for the development of northern hemisphere cyclothems? Geol. Soc. Am. Spec. Pap. 370, 5–24.
Isbell, J.L., Henry, L.C., Gulbranson, E.L., Limarino, C.O., Fraser, M.L., Koch, Z.L., Ciccioli, P.L., Dineen, A.A., 2012. Glacial paradoxes during the LPIA: evaluating the equilibrium line altitude as a control on glaciation. Earth Sci. Rev. 22, 1–19.
Isbell, J.L., Biakov, A.S., Verdernikov, I.L., Davydov, V.I., Gulbranson, E.L., Fedorchuk, N.D., 2016. Permian diamictites in northeastern Asia: Their significance concerning the bipolarity of the late Paleozoic ice age. Earth Sci. Rev. 154, 279–300.
Isbell, J.L., Koch, Z.J., Szablewski, G.M., Lenaker, P.A., 2008a. Permian glaciogenic deposits in the Transantarctic Mountains, Antarctica. In: Fielding, C.R., Frank, T. D., Isbell, J.L. (Eds.), Resolving the Late Paleozoic Ice Age in Time and Space. Geological Society of America Special Publication 441, 59-70.
Isbell, J.L., Cole, D.I., Catuneanu, O., 2008b. Carboniferous-Permian glaciation in the main Karoo Basin, South Africa: stratigraphy, depositional controls, and glacial dynamics. In: Fielding, C.R., Frank, T.D., Isbell, J.L. (Eds.), Resolving the Late Paleozoic Ice Age in Time and Space. Geol. Soc. Am. Spec. Pap. 441, 71-82.
Isbell, J.L., Vesely, F.F., Rosa, E.L., Pauls, K.N., Fedorchuk, N.D., Ives, L.R., McNall, N.B., Litwin, S.A., Borucki, M.K., Malone, J.E., Kusick, A.R., 2021. Evaluation of physical and chemical proxies used to interpret past glaciations with a focus on the late Paleozoic Ice Age. Earth-Sci. Rev. 221, 103756.
Isbell, J.L., Fedorchuk, N.D., Rosa, E.L.M., Goso, C., Alonso-Muruaga, P.J., 2023. Reassessing a glacial landscape developed during terminal glaciation of the Late Paleozoic Ice Age in Uruguay. Sediment. Geol. 451, 106399.
Ives, L.R., Isbell, J.L., Licht, K.J., 2022. A "Local First" approach to glacigenic sediment provenance demonstrated using U-Pb detrital zircon geochronology of the Permo-Carboniferous Wynyard Formation, Tasmanian Basin. The Sedimentary Record 20, 1–14.
Kay, S.M., Orrel, S., Abbruzzi, J.M., 1996. Zircon and whole rock Nd-Pb isotopic evidence for a Grenville age and Laurentian origin for the basement of the Precordillera terrane in Argentina. J. Geol. 104, 637–648.
Keller, M., 1999. Argentine Precordillera: sedimentary and plate tectonic history of a Laurentian crustal fragment in South America. Geol. Soc. Am. Spec. Pap. 341, 131.
Keller, M., Buggisch, W., Lehnert, O., 1998. The stratigraphical record of the Argentine Precordillera and its plate-tectonic background. Geol. Soc. London Spec. Pub. 142, 35–56.
Kissock, J.K., Finzel, E.S., Malone, D.H., Craddock, J.P., 2018. Lower-Middle Pennsylvanian strata in the North American midcontinent record the interplay between erosional unroofing of the Appalachians and eustatic sea-level rise. Geosphere 14, 141–161.
Kneller, B., Milana, J.P., Buckee, C., Al Jaaidi, O.S., 2004. A depositional record of deglaciation in a paleofjord (Late Carboniferous [Pennsylvanian] of San Juan Province, Argentina); the role of catastrophic sedimentation. Geol. Soc. Am. Bull. 116, 348–367.
Larrovere, M.A., Casquet, C., Aciar, R.H., Baldo, E.G., Alasino, P.H., Rapela, C.W., 2021. Extending the Pampean orogen in western Argentina: New evidence of Cambrian magmatism and metamorphism within the Ordovician Famatinian belt revealed by new SHRIMP U-Pb ages. J. S. Am. Earth Sci. 109, 103222.
Limarino, C.O., Cesari, S.N., Net, L.I., Marenssi, S.A., Gutierrez, P.R., Tripaldi, A., 2002. The Upper Carboniferous postglacial transgression in the Paganzo and Río Blanco Basins (northwestern Argentina): facies and stratigraphic significance. J. S. Am. Earth Sci. 15, 445–460.
Limarino, C.O., Alonso-Muruaga, P.J., Ciccioli, P.L., Perez Loinaze, V.S., Césari, S.N., 2014a. Stratigraphy and palynology of a late Paleozoic glacial paleovalley in the Andean Precordillera, Argentina. Palaeogeogr. Palaeoclimatol. Palaeoecol. 412, 223–240.
Limarino, C.O., Césari, S.N., Spalletti, L.A., Taboada, A.C., Isbell, J.L., Geuna, S., Gulbranson, E.L., 2014b. A paleoclimatic review of southern South America during the late Paleozoic: a record from icehouse to extreme greenhouse conditions. Gondw. Res. 25, 1396–1421.
Limarino, C.O., Gaido, M.F., Cegarra, M.I., Anselmi, G., 2011. Evolucion paleoambiental y correlacion regional de la Formacion Ansilta (Precordillera Occidental de San Juan). In: Resumenes en XVIII Congreso Geologico Argentino. Neuquen.
Limarino, C., Gutierrez, P., 1990. Diamictites in the Agua Colorada Formation (northwestern Argentina): New evidence of Carboniferous glaciation in South America. J. S. Am. Earth Sci. 3, 9–20.
Limarino, C., Tripaldi, A., Marenssi, S., Fauqué, L., 2006. Tectonic, sea-level, and climatic controls on late Paleozoic sedimentation in the western basins of Argentina. J. S. Am. Earth Sci. 33, 205–226.
López-Gamundí, O.R., 1986. Turbiditas en la sección basal de la Formación Ansilta, Paleozoico Superior De La Precordillera Occidental. Provincia De San Juan: Revista De La Asociacion Geologica Argentina 41, 106–116 (in Spanish).
López-Gamundi, O.R., 1987. Depositional models for the glaciomarine sequences of Andean Late Paleozoic basin of Argentina. Sed. Geol. 52, 109–126.
López-Gamundí, O.R., 1997. Glacial-postglacial transition in the Late Paleozoic basins of southern South America. In: Martini, I.P. (Ed.), Late Glacial and Postglacial Environmental Changes: Quaternary, Carboniferous-Permian, and Proterozoic. Oxford University Press, Oxford, pp. 147–168.
López-Gamundí, O.R., Azcuy, C.L., Cuerda, A., Valencio, D.A., Vilas, J.F., 1987. Cuencas Rio Blanco y Calingasta-Uspallata. El Sistema Carbonífero en la República Argentina. Córdoba, Nacional De Ciencias De Córdoba. 101–132 (in Spanish).
López-Gamundi, O.R., Buatois, L.A., 2010. Late Paleozoic glacial events and postglacial transgressions in Gondwana. Geol. Soc. Am. Spec. Pap. 468, 5–8.
López-Gamundí, O.R., Espejo, I.S., Conaghan, P.J., Powell, C.M., Veevers, J.J., 1994. Southern South America. Geol. Soc. Am. Mem. 184, 281–329.
López-Gamundí, O., Limarino, C.O., Isbell, J.L., Pauls, K., Césari, S.N., Alonso Muruaga, P., 2021. The late Paleozoic Ice Age along the southwestern margin of Gondwana: Facies models, age constraints, correlation, and sequence stratigraphic framework. J. S. Am. Earth Sci. 107, 103056.
López-Gamundí, O.R., Martínez, M., 2003. Esquema estratigráfico-secuencial para las unidades neopaleozoicas de la cuenca Calingasta-Uspallata en el flanco occidental de la Precordillera. Rev. Asoc. Geol. Argent. 58, 367–382 (in Spanish).
López-Gamundí, O.R., Sterren, A.F., Cisterna, G.A., 2016. Inter-and intra-till boulder pavements in the Carboniferous Hoyada Verde Formation of West Argentina: An insight on glacial advance/retreat fluctuations in Southwestern Gondwana. Palaeogeogr. Palaeoclimatol. Palaeoecol. 447, 29–41.
Malkowski, M.A., Sharman, G.R., Johnstone, S.A., Grove, M.J., Kimbrough, D.L., Graham, S.A., 2019. Dilution and propagation of provenance trends in sand and mud: geochemistry and detrital zircon geochronology of modern sediment from central California (USA). Am. J. Sci. 319, 846–902.
López-Gamundí, O., Martínez, M., 2000. Evidence of glacial abrasion in the Calingasta-Uspallata and western Paganzo basins, mid-Carboniferous of western Argentina. Palaeogeogr. Palaeoclimatol. Palaeoecol. 159, 145–165.
Malkowski, M.A., Johnstone, S.A., Sharman, G.R., White, C.J., Scheirer, D.S., Barth, G. A., 2022. Continental shelves as detrital mixers: U-Pb and Lu–Hf detrital zircon provenance of the Pleistocene-Holocene Bering Sea and its margins. The Depositional Record 8, 1008–1030.
Malone, J.R., Dalziel, I.W.D., Stone, P., Horton, B.K., 2023b. Provenance analysis of Paleozoic strata in the Falkland/Malvinas Islands: Implications for paleogeography and Gondwanan reconstructions. Gondw. Res., 1–21
Malone, D.H., Grimley, D.A., Gifford, J.N., Colgan, P.M., Craddock, J.P., Phillips, A.C., Meister, P.A., Lowe, T.H., Rickels, E.K., 2022. Provenance of Middle to Late Pleistocene tills in Illinois, USA: Evidence for long distance (~2000 km) ice transport during two successive glaciations. J. Sediment. Res. 92, 1044–1053.
Malone, J.E., Isbell, J.L., Taboada, A.C., Pagani, M.A., 2023a. Facies sedimentology and sequence stratigraphy of the carboniferous lower section of the Ansilta Formation, Calingasta-Uspallata Basin. NW Argentina. J. S. Am. Earth, Sci, p. 104345.
Marenssi, S.A., Tripaldi, A., Limarino, C.O., Caselli, A.T., 2005. Facies and architecture of a Carboniferous grounding-line system from the Guandacol Formation, Paganzo Basin, northwestern Argentina. Gondw. Res. 8, 187–202.
Martin, E.L., Collins, W.J., Spencer, C.J., 2020. Laurentian origin of the Cuyania suspect terrane, western Argentina, confirmed by Hf isotopes in zircon. Geol. Soc. Am. Bull. 132, 273–290.
Martin, J.R., Redfern, J., Williams, B.P.J., 2012. Evidence for multiple ice centres during the late Paleozoic ice age in Oman; outcrop sedimentology and

provenance of the Late Carboniferous-Early Permian Al Khlata Formation. Geochem. Soc. Spec. Publ. 368, 229–256.
Martin, J.R., Redfern, J., Horstwood, M.S.A., Mory, A.J., Williams, B.P.J., 2019. Detrital zircon age and provenance constraints on late Paleozoic ice-sheet growth and dynamics in Western and Central Australia. Aust. J. Earth Sci. 66, 183–207.
Martina, F., Canelo, H.N., Ávila, F.M., Hollanda, M.H.B.M., Teixeira, W., 2018. Mississippian lamprphyre dikes in western Sierras Pampeanas, Argentina: Evidence of transtensional tectonics along the SW margin of Gondwana. J. S. Am. Earth Sci. 83, 68–80.
McKenzie, N.R., Horton, B.K., Loomis, S.E., Stockli, D.F., Planavsky, N.J., Lee, C.T.A., 2016. Continental arc volcanism as the principal driver of icehouse-greenhouse variability. Science 352, 444–447.
Milana, J.P., Bercowski, F., 1993. Late Paleozoic glaciation in Paganzo Basin, western Argentina: sedimentological evidence. In Compte Rendus XII Congres International Stratigraphie Et Geologie Du Carbonifere Et Permien 1, 325–335.
Milana, J.P., Di Pasquo, M., 2019. New chronostratigraphy for a lower to upper Carboniferous strike-slip basin of W-Precordillera (Argentina): Paleogeographic, tectonic, and glacial importance. J. S. Am. Earth Sci. 96, 102383.
Milana, J.P., Di Pasquo, M., 2023. Carboniferous marine deposits of the Tontal section suggest that no Protoprecordillera existed along the Western Gondwana margin. Sed. Geol. 454, 106458.
Montañez, I.P., 2022. Current synthesis of the penultimate icehouse and its imprint on the Upper Devonian through Permian stratigraphic record. Geol. Soc. London Spec. Pub. 512, 213–245.
Montañez, I.P., Poulsen, C.J., 2013. The Late Paleozoic Ice Age: an evolving paradigm. Annu. Rev. Earth Planet. Sci. 41, 629–656.
Montañez, I.P., McElwain, J.C., Poulsen, C.J., White, J.D., DiMichele, W.A., Wilson, J.P., Griggs, G., Hren, M.T., 2016. Climate, pCO_2 and terrestrial carbon cycle linkages during late Palaeozoic glacial–interglacial cycles. Nat. Geosci. 9, 824–828.
Moreno, J.A., Dahlquist, J.A., Cámera, M.M.M., Alasino, P.H., Larrovere, M.A., Basei, M. A., Galindo, C., Zandomeni, P.S., Rocher, S., 2020. Geochronology and geochemistry of the Tabaquito batholith (Frontal Cordillera, Argentina): geodynamic implications and temporal correlations in the SW Gondwana margin. J. Geol. Soc. 177, 455–474.
Mory, A., 2017. A Paleozoic Perspective of Western Australia. Geological Survey of Western Australia, Perth, Western Australia.
Mottin, T.E., Vesely, F.F., Lima Rodrigues, M.C.N., Kipper, F., Souza, P.A., 2018. The paths and timing of late Paleozoic ice revisited: New stratigraphic and paleo-ice flow interpretations from a glacial succession in the upper Itararé Group (Paraná Basin, Brazil). Palaeogeogr. Palaeoclimatol. Palaeoecol. 490, 488–504.
Mottin, T.E., Vesely, F.F., Iannuzzi, R., Griffis, N.P., Montañez, I.P., 2023. Spatiotemporal variability of the late Paleozoic glacial-to-postglacial transition across eastern Paraná Basin, Brazil. Sediment. Geol. 453, 106420.
Moxness, L.D., Isbell, J.L., Pauls, K.P., Limarino, C.O., Schencman, J., 2018. Sedimentology of the mid-Carboniferous fill of the Olta paleovalley, eastern Paganzo Basin, Argentina: Implications for glaciation and controls on diachronous deglaciation in western Gondwana during the late Paleozoic Ice Age. J. S. Am. Earth Sci. 84, 127–148.
Naipauer, M., Vujovich, G.I., Cingolani, C.A., McClelland, W.C., 2010. Detrital zircon analysis from the Neoproterozoic-Cambrian sedimentary cover (Cuyania terrane), Sierra de Pie de Palo, Argentina: Evidence of a rift and passive margin system? J. S. Am. Earth Sci. 29, 306–326.
Pankhurst, R.J., Rapela, C.W., Saavedra, J., Baldo, E., Dahlquist, J., Pascua, I., Fanning, C.M., 1998. The Famatinian magmatic arc in the Central Sierras Pampeanas: An early to mid-Ordovician continental arc on the Gondwana margin. In: Pankhurst, R.J., Rapela, C.W. (Eds.), The Proto-Andean Margin of Gondwana, 142. Geological Society of London Special Publication, 343–367.
Pankhurst, R.J., Rapela, C.W., Fanning, C.M., 2000. Age and origin of coeval TTG, I- and S-type granites in the Famatinian belt of NW Argentina. Earth Env. Sci. T. R. Soc. 91, 151–168.
Pauls, K.N., 2020. Late Paleozoic climatic reconstruction of western Argentina: glacial extent and deglaciation of southwestern Gondwana. University of Wisconsin-Milwaukee, Milwaukee, WI, Department of Geosciences, p. 291.
Pauls, K.N., Isbell, J.L., McHenry, L., Limarino, C.O., Moxness, L.D., Schencman, L.J., 2019. A paleoclimatic reconstruction of the Carboniferous-Permian paleovalley fill in the eastern Paganzo Basin: Insights into glacial extent and deglaciation of southwestern Gondwana. J. S. Am. Earth Sci. 95, 102236.
Pauls, K.N., Isbell, J.L., Limarino, C.O., Alonso-Murauga, P.J., Malone, D.H., Schencman, L.J., Colombi, C.E., Moxness, L.D., 2021. Constraining late Paleozoic ice extent in the Paganzo basin of western Argentina: Provenance of the lower Paganzo group strata. J. S. Am. Earth Sci. 106, 102899.
Playford, G., Borghi, L., Lobato, G., Melo, J.H.G., 2012. Palynological dating and correlation of Early Mississippian (Tournaisian) diamictite sections, Parnaíba Basin, northeastern Brazil. Rev. Esp. Micropaleontol. 44, 1–22.
Pullen, A., Ibáñez-Mejia, M., Gehrels, G.E., Giesler, D., Pecha, M., 2018. Optimization of a laser ablation-single collector-inductively coupled plasma-mass spectrometer (Thermo Element 2) for accurate, precise, and efficient zircon U-Th-Pb geochronology. Geochem. Geophys. Geosyst. 19, 3689–3705.
Ramacciotti, C.D., Baldo, E.G., Casquet, C., 2015. U-Pb SHRIMP detrital zircon ages from the Neoproterozoic Difunta Correa Metasedimentary Sequence (Western Sierras Pampeanas, Argentina): Provenance and paleogeographic implications. Precambr. Res. 270, 39–49.
Ramos, V.A., 1988. The tectonics of the Central Andes; 30 to 33 S latitude. Geol. Soc. Am. Spec. Pap. 218, 31.
Ramos, V.A., 2004. Cuyania, an exotic block to Gondwana: review of a historical success and the present problems. Gondw. Res. 7, 1009–1026.
Ramos, V.A., Jordan, T.E., Allmendinger, R.W., Kay, S.M., Cortes, J.M., Palma, M.A., 1984. Chilenia: an allochthonous terrane in the Paleozoic evolution of the Central Andes. Actas Del Congreso Geológico Argentino 2, 84–106.
Ramos, V.A., Jordan, T.E., Allmendinger, R.W., Mpodozis, M.C., Kay, S.M., Cortes, J.M., Palma, M., 1986. Paleozoic terranes of the central Argentine-Chilean Andes. Tectonics 5, 855–880.
Ramos, V.A., Dallmeyer, D., Vujovich, G., Pankhurst, R., Rapela, C., 1998. Time constraints on the Early Paleozoic docking of the Precordillera, Central Argentina. Geol. Soc. London Spec. Pub. 142, 143–158.
Ramos, V.A., Escayola, M., Leal, P., Pimentel, M.M., Santos, J.O.S., 2015. The late stages of the Pampean Orogeny, Cordoba (Argentina): Evidence of post collisional Early Cambrian slab break-off magmatism. J. S. Am. Earth Sci. 351–364.
Ramos, V.A., 1999. Evolucion tectonica de la Argentina. In: Rasgos Estructurales del Territorio Argentino, vol. 29. Instituto de Geología y Recursos Minerales, Geología Argentina Anales, 24, 715–784 (in Spanish).
Rapalini, A.E., 2005. The accretionary history of southern South America from the latest Proterozoic to the late Paleozoic: Some paleomagnetic constraints. In: Vaughan, A.P. M., Leat, P.T., Pankhurst, R.J. (Eds.), Terrane Processes at the Margins of Gondwana, 246. Geological Society London Special Publication, 305–328.
Rapela, C.W., Pankhurst, R.J., Casquet, C., Baldo, E., Saavedra, J., Galindo, C., Fanning, C.M., 1998. The Pampean orogeny of the southern proto-Andes: evidence for Cambrian continental collision in the Sierras de Cordoba. In: Pankhurst, R.J., Rapela, C.W. (Eds.), The Proto-Andean Margin of Gondwana. Geological Society of London, 181–217.
Rapela, C.W., Pankhurst, R.J., Casquet, C., Fanning, C.M., Baldo, E.G., Gonzalez-Casado, J.M., Galindo, C., Dahquist, J., 2007. The Río de la Plata craton and the assembly of SW Gondwana. Earth Sci. Rev. 83, 49–82.
Rapela, C.W., Verdecchia, S.O., Casquet, C., Pankhurst, R.J., Baldo, E.G., Galindo, C., Murra, J.A., Dahlquist, J.A., Fanning, C.M., 2016. Identifying Laurentian and SW Gondwana sources in the Neoproterozoic to Early Paleozoic metasedimentary rocks of the Sierras Pampeanas: Paleogeographic and tectonic implications. Gondw. Res. 32, 193–212.
Rapela, C.W., Pankhurst, R.J., Casquet, C., Dahlquist, J.A., Fanning, M., Baldo, E.G., Galindo, C., Alasino, P.H., Ramacciotti, C.D., Verdecchia, S.O., Murra, J.A., Basei, M.A.S., 2018. A review of the Famatinian Ordovician magmatism in southern South America: evidence of lithosphere reworking and continental subduction in the early proto-Andean margin of Gondwana. Earth Sci. Rev. 187, 259–285.
Rino, S., Kon, Y., Sato, W., Maruyama, S., Santosh, M., Zhao, D., 2008. The Grenvillian and Pan-African orogens: world's largest orogenies through geologic time, and their implications on the origin of superplume. Gondw. Res. 14, 51–72.
Rocha-Campos, A.C., dos Santos, P.R., Canuto, J.R., Fielding, C.R., Frank, T.D., Isbell, J. L., 2008. Late paleozoic glacial deposits of Brazil: Paraná Basin. Resolving the late Paleozoic ice age in time and space. Geol. Soc. Am. Spec. Pap. 441, 97–114.
Rosa, E.L.M., Isbell, J.L., 2021. Late Paleozoic Glaciation. Reference Module in Earth Systems and Environmental Sciences. Elsevier, pp. 534–545.
Rosa, E.L., Vesely, F.F., Isbell, J.L., Kipper, F., Fedorchuk, N.D., Souza, P.A., 2019. Constraining the timing, kinematics and cyclicity of Mississippian-Early Pennsylvanian glaciations in the Paraná Basin, Brazil. Sediment. Geol. 384, 29–49.
Rygel, M.C., Fielding, C.R., Frank, T.D., Birgenheier, L.P., 2008. The magnitude of late Paleozoic glacioeustatic fluctuations: a synthesis. J. Sediment. Res. 78, 500–511.
Santos, J.O.S., Hartmann, L.A., Bossi, J., Campal, N., Schipilov, A., Piñeyro, D., McNaughton, N.J., 2003. Duration of the Trans-Amazonian Cycle and its correlation within South America based on U-Pb SHRIMP geochronology of the La Plata Craton, Uruguay. Int. Geol. Rev. 45, 27–48.
Saylor, J.E., Sundell, K.E., 2016. Quantifying comparison of large detrital geochronology data sets. Geosphere 12, 203–220.
Saylor, J.E., Sundell, K.E., Sharman, G.R., 2019. Characterizing sediment sources by non-negative matrix factorization of detrital geochronological data. Earth Planet. Sci. Lett. 512, 46–58.
Scalabrini Ortiz, J., 1972. El Carbónico en el sector septentrional de la Precordillera sanjuanina. Rev. Asoc. Geol. Argent. 27, 351–377 (in Spanish).
Schwartz, J.J., Gromet, L.P., Miro, R., 2008. Timing and duration of the calc-alkaline arc of the Pampean Orogeny: implications for the Late Neoproterozoic to Cambrian evolution of Western Gondwana. J. Geol. 116, 39–61.
Scotese, C.R., Barrett, S.F., 1990. Gondwana's movement over the South Pole during the Palaeozoic: evidence from lithological indicators of climate. In: McKerrow, W.S., Scotese, C.R. (Eds.), Palaeozoic Palaeogeography and Biogeography. Geological Society, London, Memoirs, 12, 75–85.
Sharman, G.R., Sharman, J.P., Sylvester, Z., 2018. DetritalPy: A Python-based toolset for visualizing and analyzing detrital geo- thermochronologic data. The Depositional Record 4, 202–215.
Shi, G.R., Waterhouse, J.B., 2010. Late Palaeozoic global changes affecting high-latitude environments and biotas: an introduction. Palaeogeogr. Palaeoclimatol. Palaeoecol. 298, 1–16.
Sial, A.N., Peralta, S., Gaucher, C., Toselli, A.J., Ferreira, V.P., Frei, R., Parada, M.A., Pimentel, M.M., Pereira, N.S., 2013. High-resolution stable isotope stratigraphy of the upper Cambrian and Ordovician in the Argentine Precordillera: Carbon isotope excursions and correlations. Gondw. Res. 24, 330–348.
Soreghan, G.S., Soreghan, M.J., Heavens, N.G., 2019. Explosive volcanism as a key driver of the late Paleozoic ice age. Geology 47, 600–604.

Starck, D., Del Papa, C., 2006. The northwestern Argentina Tarija Basin: Stratigraphy, depositional systems, and controlling factors in a glaciated basin. J. S. Am. Earth Sci. 22, 169–184.
Starck, D., Bordese, S., Guibaldo, C., Hernández, R., 2021. Size and style of the Gondwana late Paleozoic ice cover: insights from U-Pb dating of the Tarija Formation granitic boulders. J. S. Am. Earth Sci. 106, 102954.
Sundell, K.E., Gehrels, G.E., Pecha, M.E., 2021. Rapid U-Pb Geochronology by Laser Ablation Multi-Collector ICP-MS. Geostand. Geoanal. Res. 45, 37–57.
Taboada, A.C., 2004. Braquiópodos y bioestratigrafía del Carbonífero del Cordón del Naranjo (Subcuenca Calingasta-Uspallata), Argentina. Ameghiniana 41, 405–422 (in Spanish).
Taboada, A.C., 2009. An approach to the Carboniferous-Early Permian stratigraphy, paleontology, paleogeography and paleoclimatology of the Calingasta-Uspallata Subbasin (Western Argentina) and Tepuel-Genoa Basin (Patagonia, Argentina): A fieldguide. Permophiles 53, 13–48.
Taboada, A.C., 2010. Mississippian-Early Permian brachiopods from western Argentina: tools for middle-to high-latitude correlation, paleobiogeographic and paleoclimatic reconstruction. Palaeogeogr. Palaeoclimatol. Palaeoecol. 298, 152–173.
Thomas, W.A., Astini, R.A., 1996. The Argentine precordillera: a traveler from the Ouachita embayment of North American Laurentia. Science 273, 752–757.
Thomas, W.A., Astini, R.A., Mueller, P.A., McClelland, W.C., 2015. Detrital-zircon geochronology and provenance of the Ocloyic synorogenic clastic wedge, and Ordovician accretion of the Argentine Precordillera terrane. Geosphere 11, 1749–1769.
Thomas, W.A., Gehrels, G.E., Sundell, K.E., Greb, S.F., Finzel, E.S., Clark, R.J., Malone, D.H., Hampton, B.A., Romero, M.C., 2020. Detrital zircons and sediment dispersal in the eastern Midcontinent of North America. Geosphere 16, 817–843.
Trewin, N.H., Macdonald, D.I.M., Thomas, C.G.C., 2002. Stratigraphy and sedimentology of the Permian of the Falkland Islands: lithostratigraphic and palaeoenvironmental links with South Africa. J. Geol. Soc. 159, 5–19.
Valdez Buso, V., di Pasquo, M., Milana, J.P., Kneller, B., Fallgatter, C., Junior, F.C., Paim, P.S.G., 2017. Integrated U-Pb zircon and palynological/palaeofloristic age determinations of a Bashkirian palaeofjord fill, Quebrada Grande (Western Argentina). J. S. Am. Earth Sci. 73, 202–222.
Valdez Buso, V., Milana, J.P., Di Pasquo, M., Paim, P., Danielski Aquino, C., Cagliari, J., Chemale Junior, F., Kneller, B., 2020. Timing of the Late Palaeozoic glaciation in western Gondwana: New ages and correlations from Paganzo and Paraná basins. Palaeogeogr. Palaeoclimatol. Palaeoecol. 544, 109624.
Valdez Buso, V., Milana, J.P., Di Pasquo, M., Aburto, J.E., 2021. The glacial paleovalley of Vichigasta: Paleogeomorphological and sedimentological evidence for a large continental ice-sheet for the mid-Carboniferous over central Argentina. J. S. Am. Earth Sci. 106, 103066.
Veevers, J.T., Powell, C.M., 1987. Late Paleozoic glacial episodes in Gondwanaland reflected in transgressive-regressive depositional sequences in Euramerica. Geol. Soc. Am. Bull. 98, 475–487.
Verdecchia, S.O., Casquet, C., Baldo, E.G., Pankhurst, R.J., Rapela, C.W., Fanning, M., Galindo, C., 2011. Mid- to Late Cambrian docking of the Rio de la Plata Craton to southwestern Gondwana; age constraints from U-Pb SHRIMP detrital zircon ages from Sierras de Ambato and Velasco (Sierras Pampeanas, Argentina). J. Geol. Soc. London 168, 1061–1071.
Verdecchia, S.O., Murra, J.A., Baldo, E.G., Casquet, C., Pascua, I., Saavedra, J., 2014. Geoquímica de las rocas metasedimentarias del Cambrico medio al Ordovícico temprano de la Sierra de Los Llanos (Sierras Pampeanas, Argentina): Fuente de sedimentos, correlación y ambiente geotectonico. Andean Geol. 41, 380–400 (in Spanish).
Vermeesch, P., 2012. Multi-sample comparison of detrital age distributions. Chem. Geol. 341, 140–146.
Veroslavsky, G., Rossello, E.A., López-Gamundí, O., de Santa Ana, H., Assine, M.L., Marmisolle, J., Perinotto, A.D.J., 2021. Late Paleozoic tectono-sedimentary evolution of eastern Chaco-Paraná Basin (Uruguay, Brazil, Argentina, and Paraguay). J. S. Am. Earth Sci. 106, 102991.
Visser, J.N.J., 1987. The palaeogeography of part of southwestern Gondwana during the Permo-Carboniferous glaciation. Palaeogeogr. Palaeoclimatol. Palaeoecol. 61, 205–219.
Visser, J.N.J., 1989. The Permo-Carboniferous Dwyka Formation of southern Africa: Deposition by a predominantly subpolar marine ice sheet. Palaeogeogr. Palaeoclimatol. Palaeoecol. 70, 377–391.
Visser, J.N.J., 1997. A review of the Permo-Carboniferous glaciation in Africa. In: Martini, I.P. (Ed.), Late Glacial and Postglacial Environmental Changes: Quaternary, Carboniferous-Permian, and Proterozoic. Oxford University Press, Oxford, U.K., pp. 169–191.
Von Brunn, V., 1996. The Dwyka Group in the northern part of Kwazulu/Natal, South Africa: sedimentation during late Palaeozoic deglaciation. Palaeogeogr. Palaeoclimatol. Palaeoecol. 125, 141–163.
Vujovich, G.I., Ostera, H.A., 2003. Evidencias del ciclo Pampeano en el basamento del sector noroccidental de la sierra de San Luis. Rev. Asoc. Geol. Argent. 58, 541–548 (in Spanish).